

This is an Open Access document downloaded from ORCA, Cardiff University's institutional repository: <https://orca.cardiff.ac.uk/id/eprint/117411/>

This is the author's version of a work that was submitted to / accepted for publication.

Citation for final published version:

Boelen, Lies, Debebe, Bisrat, Silveira, Marcos, Salam, Arafa, Makinde, Julia, Roberts, Chrissy h., Wang, Eddie C. Y. , Frater, John, Gilmour, Jill, Twigger, Katie, Ladell, Kristin , Miners, Kelly L., Jayaraman, Jyothi, Traherne, James A., Price, David A. , Qi, Ying, Martin, Maureen P., Macallan, Derek C., Thio, Chloe L., Astemborski, Jacquie, Kirk, Gregory, Donfield, Sharyne M., Buchbinder, Susan, Khakoo, Salim I., Goedert, James J., Trowsdale, John, Carrington, Mary, Kollnberger, Simon and Asquith, Becca 2018. Inhibitory killer cell immunoglobulin-like receptors strengthen CD8+ T cell-mediated control of HIV-1, HCV, and HTLV-1. *Science Immunology* 3 (29) , eaao2892. 10.1126/sciimmunol.aao2892

Publishers page: <http://dx.doi.org/10.1126/sciimmunol.aao2892>

Please note:

Changes made as a result of publishing processes such as copy-editing, formatting and page numbers may not be reflected in this version. For the definitive version of this publication, please refer to the published source. You are advised to consult the publisher's version if you wish to cite this paper.

This version is being made available in accordance with publisher policies. See <http://orca.cf.ac.uk/policies.html> for usage policies. Copyright and moral rights for publications made available in ORCA are retained by the copyright holders.



Supplementary Material

Contents

Supplementary Methods	3
Supplementary Results	15
Annexin V and iKIR-expressing CD8 ⁺ T cells	15
HLA class I disease associations: mediated by CD8 ⁺ T cells or NK cells?.....	15
Supplementary Figures	21
Figure S1: Impact of ligands on iKIR enhancement of the <i>HLA-B*57</i> protective effect on early viral load set point.	21
Figure S2: Impact of iKIRs on the protective effect of <i>HLA-B*57</i> on longitudinal viral load.	22
Figure S3: Impact of inhibitory KIRs on the detrimental effect of <i>HLA-B*35Px</i> on longitudinal viral load.....	24
Figure S4: KIR expression by the CD8 ⁺ T cell lines ED, VTE1 and SK1.	26
Figure S5: Gating strategy to measure CD8 ⁺ T cell survival <i>in vitro</i>	27
Figure S6: Survival of primary CD4 ⁺ T cells is enhanced by iKIR ligation <i>in vitro</i>	28
Figure S7: iKIR expression on HIV-specific CD8 ⁺ T cells (data split by cohort).	29
Figure S8: iKIR expression on pentamer-positive and pentamer-negative cells	30
Figure S9: Differentiation stage of iKIR ⁺ pentamer ⁺ CD8 ⁺ T cells	31
Figure S10: Annexin V binding to iKIR ⁺ CD8 ⁺ T cells is decreased in individuals carrying the KIR ligand.....	32
Figure S11: Schematic and predictions of possible hypotheses	33
Supplementary Tables	35
Table S1: Impact of <i>KIR3DS1</i> and <i>KIR3DL1</i> in the full IAVI cohort.	35
Table S2: Influence of individual functional iKIRs, Inhibitory Score and count of Functional Inhibitory KIRs alone.	38
Table S3: Functional iKIRs enhance the protective effect of <i>HLA-B*57</i> , analysis by factor.	40
Table S4. Impact of LILRB2 –HLA class I binding on early viral load set point in IAVI.....	42
Table S5: Functional iKIRs enhance the protective effect of <i>HLA-B*57</i> on early set point viral load, even when LILRB2_B binding score and Functional <i>KIR3DL1</i> are included.	43
Table S6: Functional iKIRs have no clear impact on the detrimental effect of <i>HLA-B*35Px</i> on viral load set-point in the IAVI cohort.....	44
Table S7: Impact of Functional iKIRs on the effect of <i>HLA-B*57</i> and <i>HLA-B*35Px</i> in the US cohort when <i>KIR3DL1_h/y+Bw4-80I</i> is included as a covariate.	45
Table S8: The protective effect of <i>HLA-A*02</i> on odds of HAM/TSP in the Kagoshima cohort is driven by <i>HLA-A*02:07</i>	46
Table S9: The protective effect of <i>HLA-B*57</i> on odds of spontaneous clearance of HCV is enhanced with increasing inhibitory scores.	47
Table S10: Can the HLA class I associations studied be explained by NK-cell mediated effects? 49	

Table S11: Parameter ranges used in the mathematical model of host-pathogen dynamics..... 51
Table S12: Most frequent *HLA B-C* combinations in the IAVI cohort 52

Supplementary Methods

Subjects in immunogenetics study

IAVI (HIV-1 seroconverters). IAVI is a prospective cohort of HIV-1 seroconverters who were identified when seronegative and followed under Protocol C of the International AIDS Vaccine Initiative (22). All individuals were treatment naïve except for short-term prevention of mother-to-child transmission (these time points were excluded). Two outcome metrics were studied: early viral load set point and time to low CD4 count. An individual's "Early viral load set point" is the mean \log_{10} of viral load measurements taken between 3-9 months post infection (84 – 252 dpi); "time to low CD4 count", was defined as time from estimated date of infection to CD4 count < 350 cells/mm³. 44 individuals were missing early viral load set point information but not time to low CD4; therefore for analysis where the outcome metric was early viral load these 44 individuals were removed. All individuals who were missing HLA class I genotype or typing for *KIR2DL1*, *KIR2DL2*, *KIR2DL3*, *KIR3DL1* or *KIR3DS1* were excluded. Functional *KIR3DS1* (defined as *KIR3DS1* with HLA B alleles bearing Bw4-80I) is protective in this cohort (**Table S1**) so all individuals carrying functional *KIR3DS1* were removed so that we had a clean background with the entire cohort studied being negative for functional *KIR3DS1*. This cohort (i.e. full IAVI minus functional *KIR3DS1*) is referred to as the IAVI cohort and all analyses were performed in this reduced cohort unless otherwise specified. The IAVI cohort consisted of N=491 individuals with time to low CD4 count information and N=461 individuals with early viral load information.

IAVI – partners (HIV-1 seropositives). IAVI-partners is an HIV-1 seroprevalent cohort (N=315), the partners of the incident cases in the main IAVI cohort. All individuals were treatment naïve except for short-term prevention of mother-to-child transmission (these time points were excluded). One outcome metric was studied: median \log_{10} viral load. Neither Functional *KIR3DL1* nor Functional *KIR3DS1* had an impact in this cohort and so individuals with these gene combinations were not removed.

CHAVI. CHAVI consists of 177 HIV-1-seropositive subjects from sub-Saharan Africa. Neither *HLA-B*57* nor *HLA-B*35Px* had a significant impact on outcome and so iKIR effects in this cohort could not be analysed. No further work could be done on this cohort so it is not discussed in the main text to save space.

US. The US cohort consists of 548 individuals with known seroconversion date. The cohort is comprised of 4 subcohorts: DC Gay (59), the Multicenter Hemophilia Cohort Study (60), the San Francisco City Clinic Cohort (61) and AIDS Linked to Intravenous Experience (62). One outcome metric, time to CD4+ T cell count < 200 cells/mm³, was studied. 57.8% of subjects were white, 38.7% African American and 3.5% Hispanic/"other"; we therefore stratified by ethnicity. Amongst whites but not African Americans both Functional *KIR3DS1* (*KIR3DS1*⁺*Bw4-80I*⁺) and Functional *KIR3DL1* (*KIR3DL1*⁺*Bw4*⁺) were protective. So, when analysing whites, we excluded everyone who was Functional *KIR3DS1*-positive and included Functional *KIR3DL1* as a covariate. When analysing African Americans neither of these steps were necessary (though we also repeated analysis of African Americans with both these steps to check that weak, insignificant effects of Functional *KIR3DS1* or Functional *KIR3DL1* were not responsible for our results).

Kagoshima (HTLV-1 seropositives). The HTLV-1 cohort (N = 392) consists of individuals of Japanese origin who resided in the Kagoshima Prefecture, Japan; there are 214 HAM/TSP patients and 178 asymptomatic carriers. One HLA allele, *HLA-B**54, has been associated with increased odds of HAM/TSP, while *HLA-C**08 and *HLA-A**02 were associated with decreased odds of HAM/TSP (63). Further analysis has shown that the protective effect of *HLA-A**02 is driven by *HLA-A**02:07 (Table S8). We have previously analysed KIR effects in this cohort (21).

HCV (HCV seropositives). The HCV cohort consists of four sub-cohorts of HCV-seropositive subjects: AIDS Link to Intravenous Experience (ALIVE, N = 226) (64), Multicenter Hemophilia Cohort Study (MHCS, N = 295) (60), Hemophilia Growth and Development Study (HGDS, N = 100) (65) and a UK cohort (N = 161) (21, 27). Functional *KIR2DL3* is protective (increased odds of spontaneous clearance), so an additional analysis where this genotype was included as a covariate was also performed. We have previously analysed KIR effects in this cohort (21).

Ethics. This study was approved by the NHS Research Ethics Committee (13/WS/0064) and the Imperial College Research Ethics Committee (ICREC_11_1_2). Informed consent was obtained at the study sites from all individuals. The study was conducted according to the principles of the Declaration of Helsinki.

KIR and HLA genotyping

The IAVI, IAVI partners, Kagoshima, US and HCV cohorts were previously KIR and HLA genotyped (21, 27, 31, 63, 66, 67). We genotyped the CHAVI samples by high-throughput quantitative PCR as described in (68).

Regression

Impact of genotype on outcome was analysed by multivariate regression using R v3.0.1 (57). Continuous variables (log viral load) were analysed by linear regression, dichotomous variables (HAM/TSP and spontaneous clearance of HCV) by logistic regression and survival times (time to low CD4 count) by Cox regression using the functions `lm`, `glm` and `coxph` respectively from the base and survival packages (57, 69, 70). Local regression lines were calculated with the function `loess` from the base package. All P-values reported are two-tailed.

Covariates. Covariates which were significant predictors of outcome were identified and included in the analysis. In the case of linear regression, covariates were included by calculating the residualised viral load (i.e. subtracting the effect of these covariates from the raw viral load). In the case of logistic and Cox regression where this approach was not possible we explicitly included covariates in the model. The following covariates were significant:

<u>Cohort</u>	<u>Outcome</u>	<u>Covariates</u>
IAVI	Early viral load set point	gender
IAVI	Time to CD4<350 cells/mm ³	age at infection, HIV-1 clinic site ¹
IAVI-partners	Median viral load	gender
US (African American)	Time to CD4<200 cells/mm ³	age at infection, subcohort
US (all ethnicities)	Time to CD4<200 cells/mm ³	age at infection, ethnicity, Func <i>KIR3DL1</i>
Kagoshima	HAM/TSP	gender, age
HCV	Spontaneous clearance	hepatitis B virus seropositivity, mode of infection, SNP rs1297986, subcohort

¹HIV-1 clinic site is collinear with viral subtype but available for more subjects

Approach. The regression was performed in two different ways: by stratification and by factor. In the stratification approach the cohort was stratified into two sub-cohorts on the basis of presence or absence of the functional iKIR of interest, high or low inhibitory score or high or low functional iKIR count. The strength of the HLA association in the two strata was then analysed by performing two separate regressions in the two strata; in this way the

impact of iKIR background on the strength of the HLA class I disease association could be assessed. Alternatively, in the factor approach we introduced a covariate with different levels for HLA^- , HLA^+KIR^- and HLA^+KIR^+ and performed multivariate regression on the whole, unstratified cohort. The impact of iKIR on the strength of the HLA class I disease association could be assessed by comparing the coefficients of the two levels HLA^+KIR^- and HLA^+KIR^+ . We favour stratification as it better controls for genes in linkage with iKIR that impact on outcome: the effect of such genes will be incorporated into the baseline for the sub-cohort and not mistaken for KIR enhancement. We report results from the stratification approach in the main text and the factor approach in supplementary results. Both approaches yield very similar conclusions. HLA class I disease associations studied are summarized in **Table 4**.

Permutation test. To quantify the statistical significance of observing an enhancement of the protective $HLA-B^*57$ effect on early viral load set point in all functional iKIR subcohorts within the IAVI cohort, we randomized without replacement the KIR genotype in the cohort 10^5 times. For each randomization, we record whether the $HLA-B^*57$ effect in each of the strata was more extreme than observed. We then counted the percentage of randomizations in which more extreme results were recorded for all functional $KIR2DL1$, $KIR2DL2$ and $KIR2DL3$ strata.

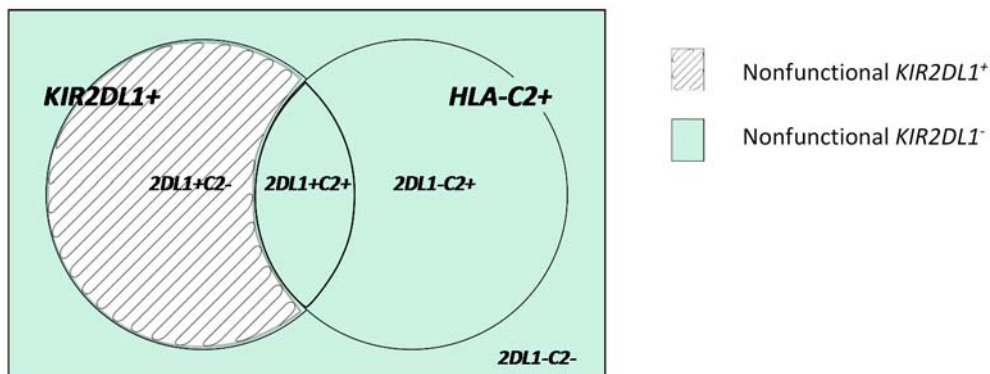
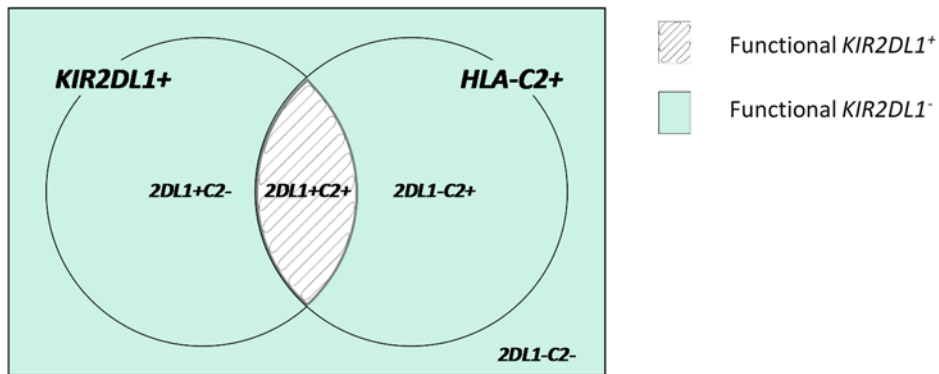
Bootstrap estimates of correlation between time and HLA effect size. For each HLA allele of interest (i.e. $HLA-B^*57$ and $HLA-B^*35Px$) 50 bootstrap samples were created by sampling with replacement from the original cohort such that there were equal numbers of individuals with low and high inhibitory score (800 HLA- and 50 HLA+) at each time interval (0,100d), (100d, 200d), (200d, 300d), (300d, 400d) and (400d, 500d). For each bootstrap sample the Spearman correlation between time and the HLA effect size (difference in loess lines between HLA+ and HLA-) was calculated separately in individuals with low and high inhibitory scores. Analysis was restricted to timepoints < 500 days to ensure sufficient cohort size. All p values reported are two-tailed.

Definitions of Functional iKIR and inhibitory score.

An individual was considered to be positive for a functional KIR if they carried both the gene for the KIR and the gene for its HLA ligand resulting in the following definitions:

Functional <i>KIR2DL1</i>	<i>KIR2DL1</i> & <i>HLA-C2</i>
Strong Functional <i>KIR2DL2</i>	<i>KIR2DL2</i> & (<i>HLA-C1</i> or <i>-B46</i> or <i>-B73</i>)
Weak Functional <i>KIR2DL2</i>	<i>KIR2DL2</i> & <i>HLA-C2</i>
Functional <i>KIR2DL3</i>	<i>KIR2DL3</i> & (<i>HLA-C1</i> or <i>-B46</i> or <i>-B73</i>)
Functional <i>KIR3DL1</i>	<i>KIR3DL1</i> & <i>HLA-Bw4</i>

Where *HLA-C1* denotes an HLA-C allele carrying a C1 motif (Asparagine at position 80); *HLA-C2* an HLA-C allele with a C2 motif (Lysine at position 80) and *HLA-Bw4* an HLA-B allele with a Bw4 motif (Asparagine at position 77). The ligands of *KIR3DL1* are contentious with one paper reporting that *KIR3DL1* binds *HLA-A*23*, *-A*24* and *-A*32* as well as *HLA-Bw4* molecules (58). If we amend our definition of Functional *KIR3DL1* to include these HLA-A alleles then the results are essentially unchanged except where noted in the text. All individuals who were not positive for a functional iKIR gene were defined as negative for that functional iKIR gene; so an individual is negative for a particular functional iKIR gene if they were missing either the KIR gene OR the gene encoding the HLA ligand. When investigating the impact of iKIR ligands (**Figure S1**) we also use the concept of “Nonfunctional iKIR”, this refers to a iKIR missing its HLA ligand. So an individual is “Nonfunctional iKIR-positive” if they have a non-functional iKIR i.e. they are positive for the iKIR but are negative for the HLA ligand. As before “nonfunctional iKIR-negative” is the complement. To illustrate the concept of functional and nonfunctional iKIR a Venn diagram is plotted below for the example of *KIR2DL1* which binds *HLA-C2*.



Definition of functional *KIR2DL1*-positive and –negative (top diagram) and non-functional *KIR2DL1*-positive and -negative (bottom diagram)

Two scores were considered: the count of the number of functional iKIR that an individual possessed and the inhibitory score which was the count adjusted for the fact that, on average, *KIR2DL2* binds C1 more strongly than it binds C2 and that, on average, *KIR2DL2* binds C1 more strongly than *KIR2DL3* binds C1. Functionally diverse alleles at the same locus (2DL2/L3 and 3DL1/S1) were scored differently to reflect different strengths of inhibitory signal.

Inhibitory score= (1 if Func 2DL1) + (1 if Strong Func 2DL2 or 0.5 if weak Func 2DL2) + (0.75 if Func 2DL3) + (1 if Func 3DL1).

When it was necessary to stratify the cohort into individuals with a high count and low count or into individuals with a high inhibitory score and a low inhibitory score we analysed all thresholds that gave a sufficiently balanced stratification (enough people in each stratum to permit analysis). In many cases the stratification provided by count of functional iKIR is the same or similar to one of the stratifications provided by inhibitory score. We report both as the count benefits from being objective (independent of our choice of weights) but the

inhibitory score is arguably more biologically relevant and benefits from a greater diversity so typically more stratifications by inhibitory score than count are possible.

In the definition of inhibitory score and inhibitory count, alleles with different binding or signalling properties were considered separately. So *KIR2DL2* and *KIR2DL3* both contributed separately as did *KIR3DL1* and *KIR3DS1* (*KIR3DS1* scoring a zero as it is activating). We also considered scores and counts in which these alleles were not counted separately vis:

Inhibitory score = (1 if Func 2DL1) + Max(1 if Strong Func 2DL2, 0.5 if weak Func 2DL2, 0.75 if Func 2DL3) + (1 if Func 3DL1).

Inhibitory count = 1 for each of Func 2DL1, Func 2DL2/L3, Func 3DL1

Results were very similar to those obtained with the original definition and conclusions were unchanged. In general, the same people fall into the high iKIR strata regardless of the exact definition (i.e. whether we use count, score, or the alternative count and score explained above) and so results typically do not change much under the different definitions.

LILRB2-B binding scores. We assigned four LILRB2 binding scores to each subject, one per *HLA* class I locus and one combined score for all *HLA* class I loci together. Specifically, for a given subject, the LILRB2_B score (for the *HLA-B* locus) was calculated as the sum of the binding scores of the subject's two *HLA-B* alleles (24). If the binding score is missing for a particular allele then we used the mean binding score of all (4 digit) alleles which are in the same 2-digit binding group. If there were no such 4 digit alleles we assigned an NA score. Following (24), the score for all loci together was calculated as the weighted sum of the individual scores, where the *HLA-A* and *HLA-B* scores were assigned weight 1, and the *HLA-C* score was assigned weight 0.1, to reflect the difference in cell surface expression between the *HLA* alleles.

***In vitro* CD8⁺ T cell survival assay**

KIR-expressing CD8⁺ T cell lines. We generated three KIR-expressing CD8⁺ T cell lines: ED, VTE1 and SK1. CD8⁺ T cell lines were obtained from two cytomegalovirus (CMV)-seropositive donors by stimulating CD8⁺ T cells with autologous fibroblasts coated with the CMV IE-1

peptide VLEETSMVL at 10 µg/ml for 1 hr at 37°C before 2 washes to remove excess. The two parental T cell lines were FACS sorted to obtain the KIR2DL3 (ED and VTE1) and KIR3DL1 (SK1) expressing T cell lines used in this study. KIR-expressing T cell lines were maintained by stimulation with allogeneic irradiated PBMC. The phenotype of the lines is shown in **Fig S4**. Genotype of ED/SK1 donor: *A02/A24 B44/B44 C05/C05; 2DL1⁺ 2DL2⁻ 2DL3⁺ 3DL1⁺ 3DL2⁻ 2DS1⁺ 2DS2⁻ 2DS3⁻ 2DS4N⁺ 2DS5⁺ 3DS1⁺ 3DL3⁺ 2DL4⁺ 2DL5⁺ 3DP1⁺*.

KIR-expressing primary CD8⁺ T cells. Three individuals who attended the Nuffield Orthopaedic Centre (Oxford, UK) and fulfilled the modified New York criteria (71) for ankylosing spondylitis (AS) were studied. All three individuals were *HLA-B27:02/05⁺*. Heparinized venous blood (10 ml) was obtained. Informed consent was provided by all subjects, and appropriate ethical permission was obtained (COREC 06/Q1606/139).

Antibodies. We used the following directly conjugated antibodies for staining of cell surface markers: anti-CD3 (HIT3a, Biolegend), anti-CD8 (SK1, Biolegend), anti-HLA-DR (L243, Biolegend) and anti-CD38 (HIT2, Biolegend). Cells were also stained with the viability dye eFluoro 780 (eBioscience) and a violet cell tracker (either eFluor450 (eBioscience) or Violet Proliferation Dye 450 (BD)). For blocking the KIR-HLA interaction we used anti-KIR2DL2/S2/L3 (GL183 (39), R&D Biosystems), anti-KIR3DL1 (DX9, R&D Biosystems), anti-KIR3DL2 (DX31, a generous gift from Jo Phillips, DNAX Research Institute USA), anti-HLA-I (DX17 (40), BD Pharmingen), anti-B27 homodimers (HD6, produced in house (41)) or IgG1 and IgG2a isotype control antibodies (MG1-45, Biolegend). For assessing KIR expression of CD8⁺ T cells (prior to survival assay) we used anti-KIR2DL3 (180701, R&D), anti-KIR2DL2/S2/L3 (GL183 (39), R&D Biosystems), anti-KIR3DL1 (DX9, R&D Biosystems), anti-KIR3DL2 (DX31, a generous gift from Jo Phillips, DNAX Research Institute USA).

Antigen presenting cells. The Epstein Barr virus-transformed HLA-A, -B and -C deficient B cell line 721.221 (72) was used to present superantigen. Untransfected 721.221 cells and 721.221 cells transfected with HLA-C03:04, -C04:01 and -B57:01 were used.

Survival assay (CD8⁺ T cell lines). The CD8⁺ T cell lines were stained with violet cell tracker (CTV) following the manufacturer's protocol then co-cultured with APCs at a 1:1 ratio at a

final concentration of 10^6 /ml in the presence of IL-2 (15 units/mL) and staphylococcal enterotoxin E (SEE, 10ng/mL) in 96 well round bottom tissue culture plates. Antibodies to block the KIR-HLA interaction (GL183 to block KIR2DL2/S2/L3 (39), Dx9 to block KIR3DL1 or Dx17 to block class I (40) or an IgG1 isotype control) were added at a concentration of 50 μ g/mL. Cells were stained at day 5 using the antibodies listed above. Events were acquired on a FACS Canto II and analysed using Kaluza v1.5a or FlowJo. The count of live CTV⁺ and live CTV⁺CD107a⁺ cells was enumerated using CountBright Absolute Counting Beads (Invitrogen). All experiments were repeated in duplicate or triplicate.

Six conditions were investigated:

- i) with addition of SEE and untransfected 221 cells (“+221” in **Fig. 3A & 3D**)
- ii) with addition of SEE and 221 cells transfected with an HLA molecule not thought to be a ligand for the KIR under investigation (“+221:B57” and “+221:C04” for KIR2DL3, “+221:C03” and “+221:C04” for KIR3DL1 in **Fig. 3A & 3D**)
- iii) with addition of SEE and 221 cells transfected with an HLA molecule that is a ligand for the KIR under investigation (“+221:C03” for KIR2DL3, “+221:B57” for KIR3DL1 in **Fig. 3A & 3D**)
- iv) with addition of SEE and 221 cells transfected with an HLA molecule that is a ligand for the KIR under investigation and isotype control antibody (“+221:C03+IgG1” for KIR2DL3, “+221:B57+IgG1” for KIR3DL1 in **Fig. 3A & 3D**)
- v) with addition of SEE and 221 cells transfected with an HLA molecule that is a ligand for the KIR under investigation and HLA blocking antibody (“+221:C03+ α HLA-I” for KIR2DL3, “+221:B57+ α HLA-I” for KIR3DL1 in **Fig. 3A & 3D**)
- vi) with addition of SEE and 221 cells transfected with an HLA molecule that is a ligand for the KIR under investigation and KIR blocking antibody (“+221:C03+ α KIR” for KIR2DL3, “+221:B57+ α KIR” for KIR3DL1 in **Fig. 3A & 3D**)

Survival assay (PBMC). PBMC from three individuals with AS were stimulated with staphylococcal enterotoxin B (SEB) at a concentration of 100 ng/mL. Antibodies to block the KIR-HLA interaction (Dx31 to block KIR3DL2, HD6 to block B27 homodimers, an IgG1 or an IgG2a isotype control) were added at a concentration of 50 μ g/mL. Cells were stained at day 5 using the antibodies listed above. Events were acquired on a FACS Canto II and analysed

using Kaluza v1.5a. The count of live CD3⁺CD8⁺ KIR3DL2⁺ cells was enumerated using CountBright Absolute Counting Beads (Invitrogen). Six conditions were investigated:

- i) without addition of SEB (“no stimulus” in **Fig. 3C**)
- ii) with addition of SEB (“+SEB” in **Fig. 3C**)
- iii) with addition of SEB and IgG2a isotype control for α HLA (“+IgG2a” in **Fig. 3C**)
- iv) with addition of SEB and IgG1 isotype control antibody for α KIR (“+IgG1” in **Fig. 3C**)
- v) with addition of SEB and HLA blocking antibody (“+ α HLA-I” in **Fig. 3C**)
- vi) with addition of SEB and KIR blocking antibody (“+ α KIR” in **Fig. 3C**).

Survival was compared between conditions using the two tailed non-parametric Wilcoxon test. For the metaanalysis, P values were combined using Stouffer’s weighted z-test (**Fig. 3B**).

iKIR expression and virus-specific CD8⁺ T cells *ex vivo*

Subjects. HIV-1-seropositive individuals came from Protocol L of the International AIDS Vaccine Initiative (different individuals to those from protocol C studied above but recruited from the same study sites) and the John Radcliffe Hospital, UK. In both cases individuals with unsuppressed or poorly suppressed viremia were selected (with the goal of maximizing the number of virus-specific CD8⁺ T cells). HTLV-1-seropositive individuals came from the National Centre of Retrovirology, UK. All selected individuals were *HLA-A*02*⁺.

Staining. Cryopreserved PBMC from HIV-1- and HTLV-1-seropositive donors were thawed and stained with the following directly conjugated antibodies: anti-CD3 (OKT3, Biolegend), anti-CD8 (SK1, Biolegend), anti-CD28 (CD28.2, Biolegend), anti-CD45RA (H100, Biolegend), anti-KIR2DL1 (REA284, Miltenyi Biotec), anti-KIR2DL2/L3 (DX27, Biolegend), anti-KIR3DL1 (DX9, Biolegend) and anti-KIR3DL2 (539304, R&D). Live cells were distinguished with LIVE/DEAD™ Fixable Aqua Dead Cell Stain (Thermofisher Scientific). Additionally cells were stained with A2-pentamers (Proimmune) complexed with ILKEPVHGV, SLYNTVATYL, LTFGWCFKL (pooled) in the case of HIV-1⁺ individuals and LLFGYPVYV in the case in HTLV-1⁺ individuals. The fraction of CD3⁺CD8⁺ pentamer⁺ cells expressing iKIR was enumerated. Coexpression of CD45 and CD28 on the CD3⁺CD8⁺ pentamer⁺ KIR⁺ cells was also recorded.

Ethics. Written informed consent was obtained and research was conducted under the governance of the Imperial College Healthcare NHS Trust Tissue Bank, approved by the UK National Research Ethics Service (09/H0606/106, 15/SC/0089). All studies were conducted according to the principles of the Declaration of Helsinki.

Mathematical model of host-pathogen dynamics in HIV-1 infection

We constructed an ordinary differential equation (ODE) model to explore the influence of iKIRs on HIV-1 dynamics.

$$\begin{aligned}\dot{x} &= \lambda_1 + s_1 x \left(1 - \frac{x+y}{k_1}\right) - \beta xv - \mu_1 x \\ \dot{y} &= s_1 y \left(1 - \frac{x+y}{k_1}\right) + \beta xv - d_1 y z_1 - d_2 y z_2 - \mu_2 y \\ \dot{v} &= py - \mu_3 v \\ \dot{z}_1 &= \lambda_2 + s_2 y z_1 \left(1 - \frac{z_1 + z_2}{k_2}\right) - \mu_4 z_1 \\ \dot{z}_2 &= \lambda_2 + s_2 y z_2 \left(1 - \frac{z_1 + z_2}{k_2}\right) - \mu_4 z_2\end{aligned}$$

Here, x denotes the number of uninfected CD4⁺ T cells/mm³; y denotes the number of infected CD4⁺ T cells/mm³ and v is the number of free virions/mm³. We model two populations of CD8⁺ T cells, z_1 and z_2 , where the former lyse target cells more efficiently than the latter (when we study the effects of iKIRs on a protective HLA allele) or less efficiently (the case of a detrimental HLA allele). Uninfected CD4⁺ T cells die at a rate μ_1 , and are replenished by λ_1 ; they become infected at rate βv , which depends on the number of free virions; proliferation is density-dependent with rate s_1 . CD8⁺ T cells are produced at rate λ_2 their proliferation occurs at rate s_2 , is density dependent and dependent on the number of infected CD4⁺ T cells and they die at rate μ_4 . The number of free virions is linearly dependent on the number of infected cells that produce them at rate p ; free virions are cleared at rate μ_3 . Parameter ranges used are given in **Table S11**.

To assess the robustness of our results, alternative structural forms of the model and alternative parameter ranges were also considered. The alternative model terms focussed

on changes to the production terms for T cells as there is little consensus on the form of these terms in the literature. We considered the following changes:

- without the CD4⁺ and CD8⁺ T cell proliferation terms $s_1(1-(x+y)/k_1)$ and $s_2(1-(z_1+z_2)/k_2)$
- without the saturation term in the CD4⁺ and CD8⁺ T cell proliferation. That is, replacing $s_1(1-(x+y)/k_1)$ with s_1 and replacing $s_2y(1-(z_1+z_2)/k_2)$ with s_2y , similar to Li & Shu (73)
- without the saturation term in the CD4⁺ T cell proliferation. That is, replacing $s_1(1-(x+y)/k_1)$ with s_1
- without the saturation term in the CD8⁺ T cell proliferation. That is, replacing $s_2y(1-(z_1+z_2)/k_2)$ with s_2y , similar to Lim & Maini (74)
- without the constant input term for CD8⁺ T cells (i.e. $\lambda_2=0$)
- replaced the CD8⁺ T cell proliferation term $s_2(1-(z_1+z_2)/k_2)$ by $s_2yz_1/(z_1+z_2+K)$, similar to Acevedo *et al* (75)

We also considered alternative parameter ranges in cases where we felt ranges were poorly known or we had reason to believe the results might be particularly sensitive to that parameter. Specifically, we increased the value of ρ to 2000 virions/cell day, increased the upper bound of β to 10^{-3} mm³/cell/day, increased the range of d_2 (and correspondingly d_1) to 0.02-0.3 /cell day, reduced the lower bound on λ_1 to 0.1 cell/mm³/day and the upper bound to 20 cell/mm³/day, reduced the lower bound on s_2 to 0.0001/day, increased the upper bound on μ_4 to 0.1/day). In all cases the key results, namely the approximate proportion of runs showing enhancement of protective associations, the approximate proportion of runs showing enhancement of detrimental associations and how these proportions changed with the impairment of the lysis rate were remarkably constant.

Supplementary Results

Annexin V and iKIR-expressing CD8⁺ T cells

We investigated the association between Annexin V binding (as a marker of cell apoptosis) and functional iKIR expression. Specifically, for each of KIR2DL1, KIR2DL2/L3 and KIR3DL1, we quantified the fraction of KIR-expressing CD8⁺ T cells which were Annexin V-positive and then we compared the fraction between individuals within whom the ligand was present and individuals where the ligand was absent. For example, for KIR2DL1, we compared the fraction of KIR2DL1⁺ CD8⁺ T cells which were Annexin V-positive in individuals who were C2⁺ (KIR2DL1 functional) with the fraction of KIR2DL1⁺ CD8⁺ T cells which were Annexin V-positive in individuals who were C2⁻ (KIR2DL1 non-functional). 15 HCV-infected individuals and 15 healthy controls were studied. There was no difference in Annexin-V binding between HCV-infected subjects and controls ($P=0.9$, WMW) and so we pooled cases and controls, however there was a significant difference with KIR ($P=0.04$ so we considered KIRs individually and then combined the P values using Stouffer's combined P). KIR2DL2/L3 could not be analysed as there were only 2 individuals with non-functional KIR2DL2/L3. For KIR2DL1 we found that Annexin V binding was significantly decreased in people with the functional ligand (Mean in C2⁻: 25.4%, mean in C2⁺: 14.3% $P=0.027$, WMW), for KIR3DL1 there was a trend in the same direction but the difference was not significant (mean in Bw4⁻: 14.4% mean in Bw4⁺:10.1%). Combining P values we found $P=0.014$ (Stouffer's weighted z-test); suggesting that presence of the KIR ligand was associated with a reduction in cell death amongst KIR-expressing CD8⁺ T cells. Interestingly a similar observation was made for CD4⁺ T cells ($P=0.023$, Stouffer's combined P value), **Figure S10**.

HLA class I disease associations: mediated by CD8⁺ T cells or NK cells?

Our starting point in interpreting the immunogenetics analysis is that that the primary HLA class I disease associations which we study (i.e. associations between outcome and HLA-A*02:07, -C*08 and -B*54 in HTLV-1, HLA-B*57 in HCV and HLA-B*57 and -B*35Px in HIV-1) are mediated by CD8⁺ T cells. However, *a priori*, an HLA class I disease association could be attributable to the HLA molecule's role as a KIR ligand rather than its role as a T cell receptor ligand (i.e. the protective/detrimental effect could be mediated by NK cells rather than CD8⁺

T cells). If an HLA class I disease association is attributable to NK cells rather than CD8⁺ T cells then other HLA class I molecules with similar KIR binding properties would (in the context of the relevant KIRs) be expected to be similarly protective/detrimental. For example, if A*02:07 is protective in the context of HTLV-1 infection because of the KIRs which it does not bind then other HLA-A alleles which also do not bind KIR would also be expected to be protective. It is this behaviour that underlies classical KIR-HLA analyses in which combinations of KIR with their groups of cognate HLA ligands are considered e.g. (28-31, 76). This behaviour was investigated for each of the HLA class I alleles we studied. The results are detailed below & in **Table S10**; a schematic summarising potential hypotheses is provided in **Fig. S11**.

HLA-B*57 in HIV-1 infection.

*HLA-B*57* is protective in the IAVI cohort (associated with reduced early viral load set point and slow progression to low CD4 cell count). *HLA-B*57* carries the Bw4-80I epitope; it binds KIR3DL1 and there is some evidence it may also bind KIR3DS1. *HLA-B57* could therefore, *a priori*, be protective because it binds KIR3DL1 and/or KIR3DS1.

KIR3DL1

A protective effect due to binding of KIR3DL1 is unlikely in this cohort as other HLA alleles that bind KIR3DL1 are not protective in the context of *KIR3DL1*. That is, neither *KIR3DL1:Bw4* nor *KIR3DL1:Bw4_80I* are associated with low early viral load set point (*KIR3DL1:Bw4* Coeff=-0.07 P=0.4. *KIR3DL1:Bw4_80I* Coeff=+0.02 P=0.8) or time to low CD4 count (*KIR3DL1: Bw4* HR=0.96 P=0.8. *KIR3DL1:Bw4_80I* HR=1.07 P=0.6). If we include the HLA-A alleles carrying the Bw4 and Bw4_80I motif then the conclusions are unchanged (**Table S10, panel A & B**). The absence of a protective effect of *KIR3DL1:Bw4* and *KIR3DL1:Bw4_80I* is even more striking if we exclude individuals positive for *HLA-B*57* from the cohort (**Table S10, panel C & D**), suggesting that what little protection is seen with *KIR3DL1:Bw4* and *KIR3DL1:Bw4_80I* is due to the presence of *HLA-B*57* in those groups. The lack of evidence for a protective effect of *HLA-B*57* attributable to *KIR3DL1* is consistent with a recent report in which, of the *B*57* alleles, only *B*57:01* (which is essentially absent from our cohort, N=1) was significantly associated with protection in the context of a noncoding mutation in *KIR3DL1* (77).

KIR3DS1

The *HLA-B*57* protective effect which we study is, by definition, independent of the effect of KIR3DS1 as all individuals with *KIR3DS1:HLA-B57* have been removed from the IAVI cohort to

prevent confounding. This does not rule out the possibility that *KIR3DS1* with *Bw4_80I* is protective but the effect that we are studying is clearly distinct.

***HLA-B*35Px* in HIV-1 infection.**

*HLA-B*35Px* is detrimental in the IAVI cohort (associated with an increased early viral load set point, but no effect on progression to low CD4 cell count). Within the IAVI cohort two alleles, *B*35:02* and *B*53:01*, constitute the *HLA-B*35Px* group. Identifying whether the *HLA-B*35Px* detrimental effect is attributable to the KIR binding properties of *HLA-B*35Px* is problematic since *HLA-B*35:02* and *HLA-B*53:01* have very different KIR binding properties (*B*35:02* carries a *Bw6* motif and *B*53:01* carries a *Bw4-80I* motif). We therefore first sought to ascertain the protective/detrimental effects of *B*53:01* and *B*35:02* on early viral load set point.

HLA	Coeff	P val	sig	N carriers	N non-carriers
<i>B*35Px</i>	+0.35	0.00066	***	78	383
<i>B*35:02</i>	+0.18	0.71115		3	458
<i>B*53:01</i>	+0.35	0.00073	***	75	386

It is clear that, within the IAVI cohort, the detrimental effect of *HLA-B*35Px* is attributable to *HLA-B*53:01* (there are only 3 subjects with *HLA-B*35:02* and it is more weakly detrimental than *HLA-B*53:01*; Coeff=+0.18 and Coeff=+0.35 resp.). We therefore investigated whether the KIR binding of *HLA-B*53:01* could explain its detrimental effects. *HLA-B*53:01* is predicted to bind *KIR3DL1* and potentially *KIR3DS1*. We therefore investigated whether its detrimental effects could be attributed to binding either of these KIR.

KIR3DL1

The detrimental effect of *HLA-B*53:01* on early viral load set point is unlikely to be attributable to its binding of *KIR3DL1* as other alleles that bind *KIR3DL1* are not detrimental in the context of *KIR3DL1*. That is, neither *KIR3DL1:Bw4* nor *KIR3DL1:Bw4_80I* are significantly associated with high early viral load set point (*KIR3DL1:Bw4* Coeff=-0.07 P=0.4. *KIR3DL1:Bw4_80I* Coeff=+0.02 P=0.8); **Table S10 panel A.**

KIR3DS1

As for *HLA-B*57*, we can be confident that the detrimental effects of *HLA-B*53:01* which we study are not attributable to *KIR3DS1* since, in the cohort we study, individuals with functional *KIR3DS1* have been removed and therefore the detrimental effect of *HLA-B*53:01* (and *HLA-B*35Px*) occurs in the absence of *KIR3DS1*.

***HLA-A*02:07* in HTLV-1 infection**

*HLA-A*02:07*, which is protective in the context of HTLV-1 infection, is not thought to contain any KIR binding motifs. To test the hypothesis that *HLA-A*02:07*-associated protection is explained by its KIR binding behaviour we therefore sought to test whether other *HLA-A* alleles that do not bind KIR are protective. We studied all non-KIR binding *HLA-A* alleles which were frequent in our cohort (carried by 30 or more individuals); analysis was conducted at the 4 digit level for direct comparability with the *A*02:07* analysis. It is clear from the results (**Table S10, panel E**) that simply failing to bind KIR does not make a protective allele. Some *HLA-A* alleles tend to be protective, some tend to be detrimental; none (other than *A*02:07*) are significant even though all are more frequent than *A*02:07*. We conclude that the protection afforded by *HLA-A*02:07* cannot be explained by its failure to bind KIR.

***HLA-C*08* in HTLV-1 infection**

*HLA-C*08* is protective in the context of HTLV-1 infection. *HLA-C08* alleles contain a C1 binding motif and as such are expected to bind *KIR2DL2/L3* and *KIR2DS2*. All individuals are positive for at least one of these KIRs. If *HLA-C*08* is protective because of its KIR binding properties then we would expect other *HLA C* alleles with the same KIR binding properties to be similarly protective in the presence of their ligating KIR. We therefore tested, for all C1 group alleles that were sufficiently frequent ($n \geq 30$) whether or not they were protective. Analysis was conducted at the 2 digit level for comparability with the *HLA-C*08* result; *HLA* alleles that are exceptions at the two digit level were excluded from the grouping (e.g. most *HLA-C*03* alleles carry a C1 motif but *C*03:07* is an exception, so someone was not counted as carrying a group C1 C03 allele if they were *HLA-C*03:07⁺*). It is clear from the results (**Table S10, panel F**) that there is no consistent picture, some of the C1 alleles tend towards protection and others tend towards susceptibility, lack of evidence for protection is not attributable to frequency as the numbers in both arms of the analysis are large for all alleles. We conclude that the protection afforded by *HLA-C*08* is unlikely to be due to its KIR binding properties.

HLA-B*54 in HTLV-1 infection

*HLA-B*54* which is detrimental in the context of HTLV-1 infection, is a Bw6 allele and not thought to contain any KIR binding motifs. To test the hypothesis that HLA-B*54-associated susceptibility is explained by its KIR binding behaviour we therefore tested whether, in general, Bw6 alleles are detrimental. We studied all HLA-B alleles with a Bw6 motif, which were frequent in our cohort (carried by 30 or more individuals). It can be seen that there is no consistent picture (**Table S10, panel G**), some of the Bw6 groups tend towards protection and others tend towards susceptibility, lack of evidence is not attributable to frequency as the numbers in both arms of the analysis are large for all alleles. We conclude that the susceptibility associated with HLA-B*54 is unlikely to be due to its inability to bind KIRs.

HLA-B*57 in HCV infection

*HLA-B*57* is protective in the context of HCV infection as it is significantly associated with an increased odds of spontaneous clearance. HLA-B*57 carries the Bw4-80I epitope, it binds KIR3DL1 and may also bind KIR3DS1. HLA-B*57 could therefore be protective because it binds KIR3DL1 and/or KIR3DS1.

KIR3DL1

A protective effect due to binding of KIR3DL1 is unlikely as other alleles that bind KIR3DL1 are not protective in the context of KIR3DL1. That is, neither *KIR3DL1:Bw4* nor *KIR3DL1:Bw4_80I* are associated with spontaneous clearance (*KIR3DL1:Bw4* OR=1.06 P=0.7. *KIR3DL1:Bw4_80I* OR=1.13 P=0.5). Extension of the definition of binding alleles to include the A alleles does not change the conclusions (**Table S10, panel H**).

KIR3DS1

A protective effect due to binding of KIR3DS1 is unlikely as other alleles that bind KIR3DS1 are not protective in the context of KIR3DS1. That is, neither *KIR3DS1:Bw4* nor *KIR3DSL1:Bw4_80I* are associated with spontaneous clearance (*KIR3DS1:Bw4* OR=1.08 P=0.7. *KIR3DL1:Bw4_80I* OR=1.24 P=0.4). Extension of the definition of binding alleles to include the A alleles does not change the conclusions (**Table S10, panel I**).

This analysis suggests that it is unlikely that any of the 6 HLA class I disease associations which we study in our patient cohorts are explained by the KIR binding properties of the HLA molecules. This is consistent with existing work using independent approaches, which indicates that these particular HLA associations are likely to be attributed to CD8⁺ T cells, see for example (32-37). We do not rule out an involvement of NK cells in determining CD8⁺ T cell survival (see Discussion & **Fig. S11**). Additionally, there is evidence for NK cell only (i.e. CD8⁺ T cell-independent effects) in controlling virus infection, e.g. *KIR3DLS1:Bw4_80I* in HIV-1 or *KIR2DL3:C1* in HCV but these effects are distinct from, and in addition to, the enhancements of HLA class I disease associations which we report.

Supplementary Figures

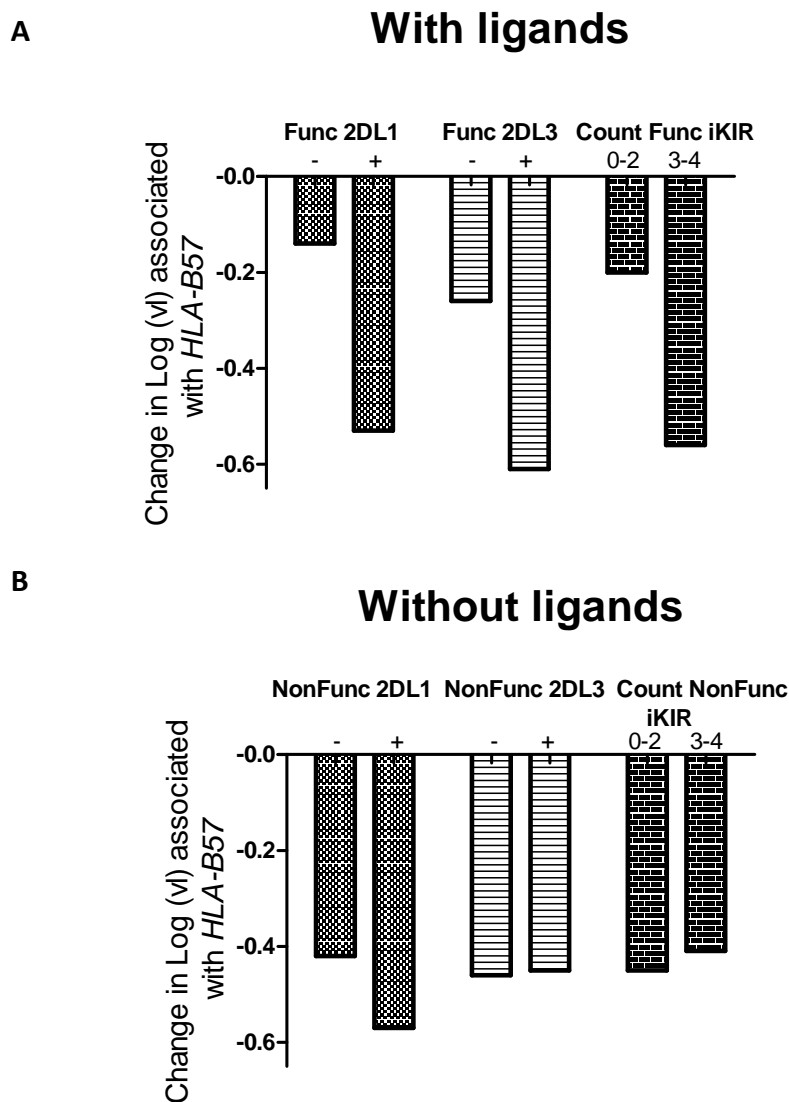


Figure S1: Impact of ligands on iKIR enhancement of the *HLA-B*57* protective effect on early viral load set point.

When ligands are included (“Functional iKIR”) panel **A**, it is seen that iKIR enhance the protective effect of *HLA-B*57*, when ligands are excluded (“NonFunctional iKIR”) panel **B** the enhancement is no longer seen. KIR2DL2 has been excluded from this analysis since its ligands are always present, inhibitory score is excluded since this cannot be defined in the absence of ligands. For the KIRs that could be studied (*KIR2DL1*, *KIR2DL3*, count of iKIR) it can be seen that the enhancement of the *HLA-B*57* protective effect by iKIR is dependent on the presence of the KIR ligands. Definitions: Func 2DL1⁺: 2DL1⁺C2⁺. Func 2DL1⁻: 2DL1⁻ or C2⁻. Func 2DL3⁺: 2DL3⁺C1⁺. Func 2DL3⁻: 2DL3⁻ or C1⁻. NonFunc 2DL1⁺: 2DL1⁺C2⁻. NonFunc 2DL1⁻: 2DL1⁺C2⁺ or 2DL1⁻. NonFunc 2DL3⁺: 2DL3⁺C1⁻. NonFunc 2DL3⁻: 2DL3⁺C1⁺ or 2DL3⁻. See **Supplementary Methods** for further details on definition of Functional and NonFunctional iKIR.

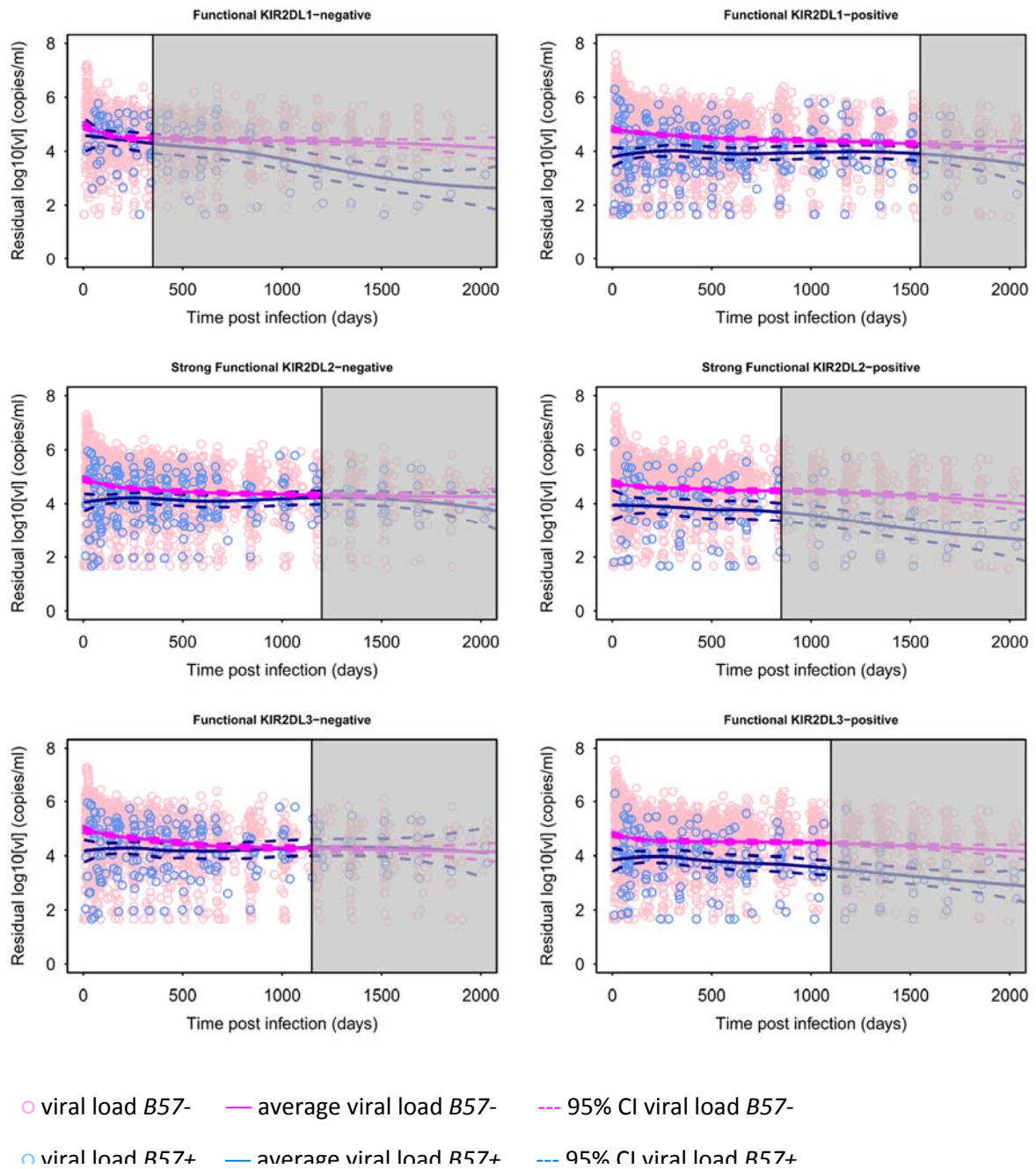


Figure S2: Impact of iKIRs on the protective effect of *HLA-B*57* on longitudinal viral load.

The IAVI cohort was stratified by presence (right hand column) or absence (left hand column) of iKIR with genes for their ligands (first row: functional *KIR2DL1*, second row: strong functional *KIR2DL2*, third row: functional *KIR2DL3*). The (residualised) viral load in *HLA-B*57*⁺ (blue circles) and *HLA-B*57*⁻ (pink circles) individuals is plotted against time. The local non-parametric regression (loess) lines are shown for *HLA-B*57*⁺ (blue) and *HLA-B*57*⁻ (pink) with 95% confidence intervals (dashed lines). The black vertical lines mark the time at which the

number of individuals in either arm drops to 10, loess lines to the right of this (i.e. in the grey shaded areas) are unreliable and should be ignored. The figures consistently show that in the presence of functional iKIR, the protective effect of *HLA-B*57* on viral load was sustained over time (that is the loess lines for *HLA-B*57+* and *HLA-B*57-* are outside each other's 95% CI). In contrast, in the absence of functional iKIR, the protective effect of *HLA-B*57* on viral load was weak. Interesting, in the absence of a strong inhibitory signal it appeared that the protective effect of *HLA-B*57* was observable at very early time points post infection but was eroded as time progressed. Viral load is residualised for gender, plots made with raw viral load are visually indistinguishable.

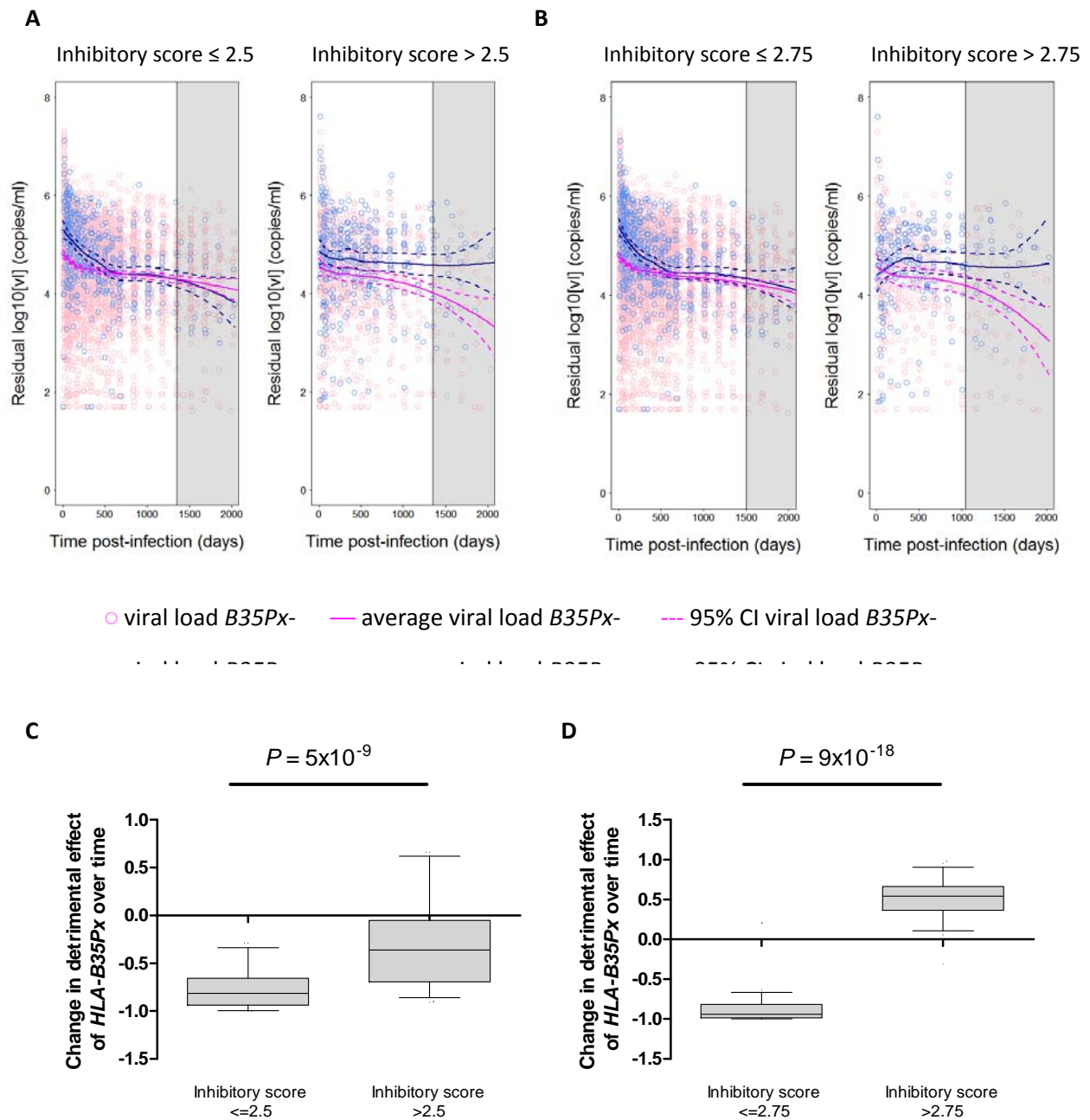


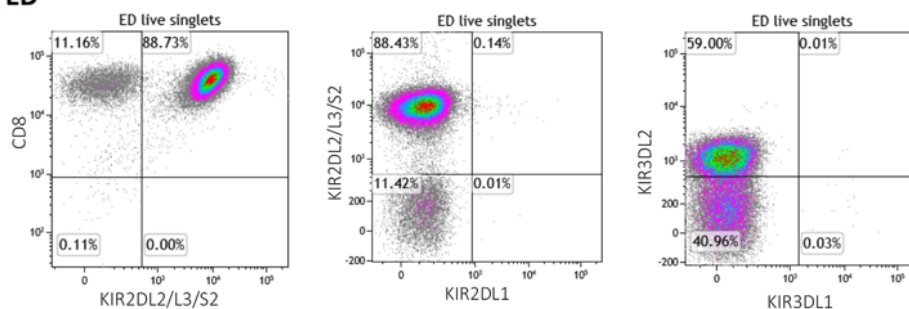
Figure S3: Impact of inhibitory KIRs on the detrimental effect of *HLA-B*35Px* on longitudinal viral load.

The IAVI cohort was stratified into individuals with a low inhibitory score (left) and individuals with a high inhibitory score (right) for a cut off of 2.5 (panel **A**) and 2.75 (panel **B**). The viral load in *HLA-B*35Px*⁺ (blue circles) and *HLA-B*35Px*⁻ (pink circles) individuals is plotted against time. The local non-parametric regression (loess) lines are shown for *HLA-B*35Px*⁺ (blue) and *HLA-B*35Px*⁻ (pink) with 95% confidence intervals (dashed lines). The black vertical lines mark

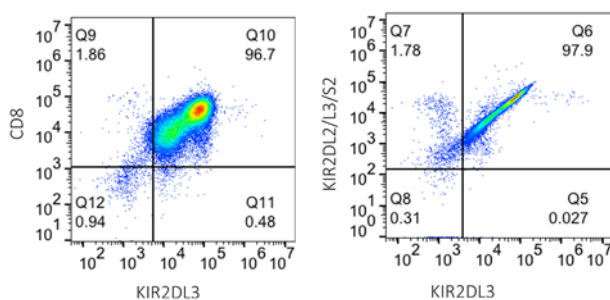
the time at which the number of individuals drops to 10, loess lines to the right of this (in grey shaded area) are unreliable and should be ignored. In the presence of a strong inhibitory signal the detrimental effect of *HLA-B*35Px* on viral load was sustained over time (that is the loess lines for *HLA-B*35Px*⁺ and *HLA-B*35Px*⁻ are outside each other's 95% CI). In contrast, in the absence of a strong inhibitory signal, although the detrimental effect of *HLA-B*35Px* on viral load can clearly be seen at early time points post infection, the detrimental effect is eroded as time progressed. Viral load is residualised for gender, plots made with raw viral load are visually indistinguishable.

Bootstrap estimation of the correlation between the *HLA-B*35Px* detrimental effect and time in the low inhibitory score strata (left box) and high inhibitory score strata (right box) for a cut off of 2.5 (panel **C**) and 2.75 (panel **D**). The detrimental effect of *HLA-B*35Px* decreased significantly more rapidly in people with a low iKIR score ($P=5 \times 10^{-9}$, 9×10^{-18} respectively). Similar results were seen for a cut-off of 2.0 ($P=6 \times 10^{-7}$).

ED



VTE1



SK1

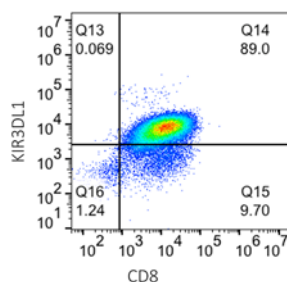


Figure S4: KIR expression by the CD8⁺ T cell lines ED, VTE1 and SK1.

In the case of ED, the antibody used to stain for KIR2DL2/S2/L3 expression (GL183) does not distinguish between KIR2DL2, KIR2DS2 and KIR2DL3. Distinction was made on the basis of genotype (donor is *KIR2DL2-KIR2DL3+KIR2DS2-*) and confirmed by mRNA expression (data not shown). In the case of VTE1 a KIR2DL3-specific antibody was used (180701); costaining with the KIR2DL2/L3/S2 antibody is also shown.

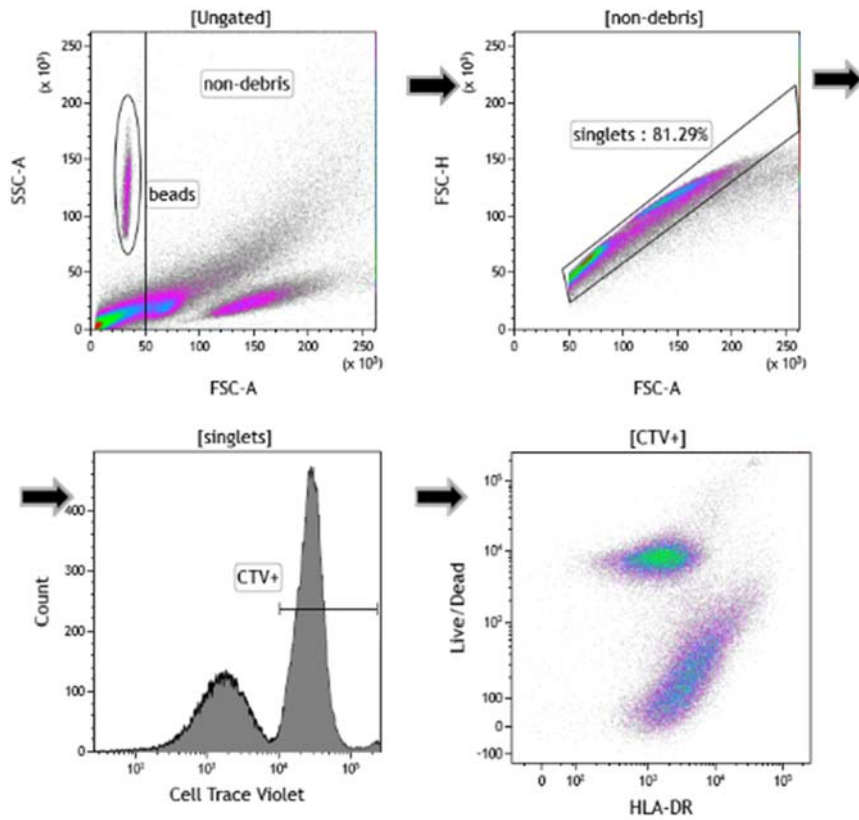


Figure S5: Gating strategy to measure CD8⁺ T cell survival *in vitro*.

Successive panels illustrate the gating strategy. Data from a representative experiment.

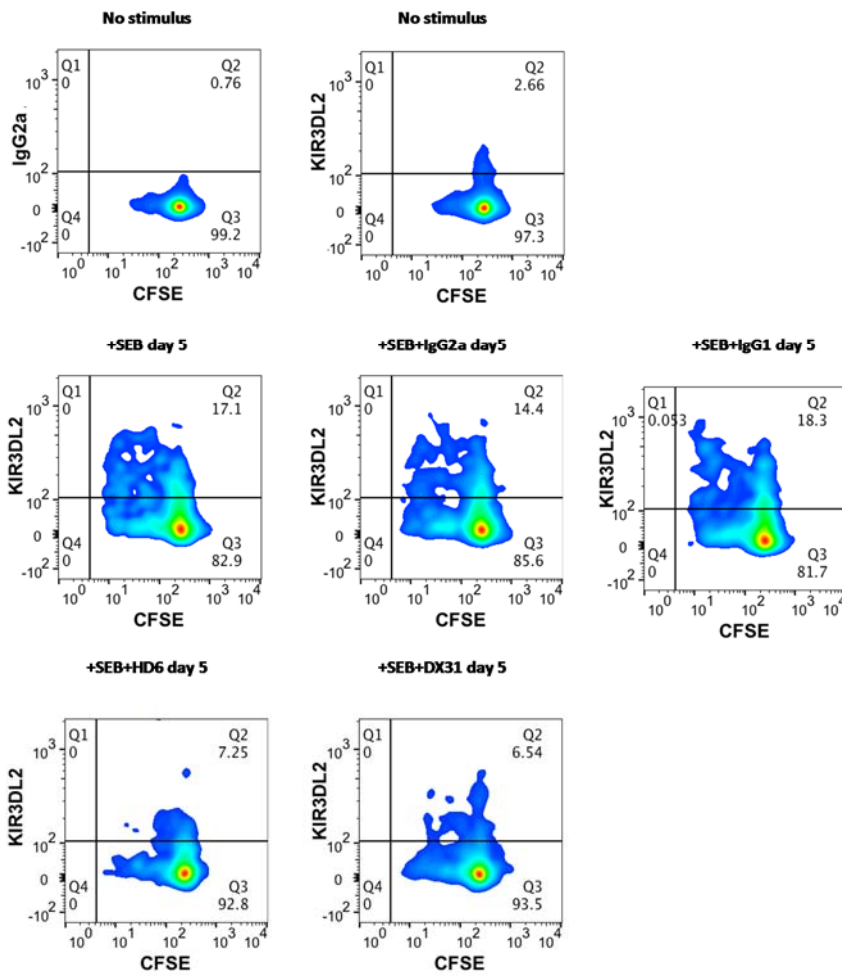


Figure S6: Survival of primary CD4⁺ T cells is enhanced by iKIR ligation *in vitro*

The impact of KIR3DL2 ligation on CD4⁺ T cells in PBMCs from *HLA-B27⁺* individuals with ankylosing spondylitis was investigated in a 5 day survival assay. Data from a representative experiment are shown. Results from all individuals are summarised in **Figure 3C**.

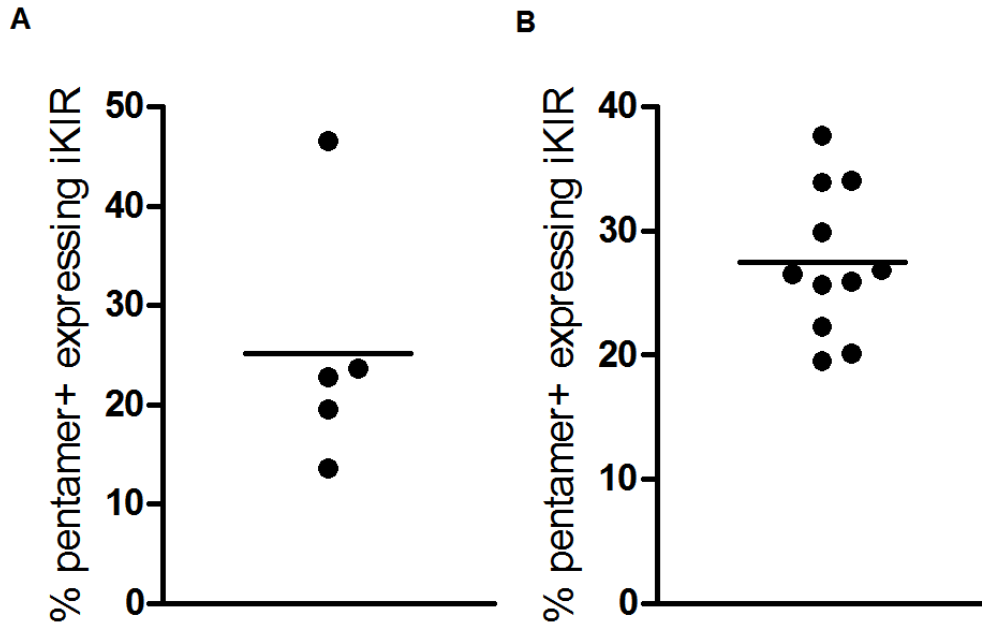


Figure S7: iKIR expression on HIV-specific CD8⁺ T cells (data split by cohort).

Virus-specific CD8⁺ T cells were identified by HLA-A2 pentamer staining in PBMC from HIV-1-seropositive individuals. The fraction of pentamer⁺ cells gated on bulk CD8⁺CD3⁺ cells expressing iKIR (KIR2DL1, KIR2DL2/L3, KIR3DL1, KIR3DL2) is plotted. The HIV-1-seropositive subjects derive from two cohorts **(A)** a South and East African cohort (same clinic centres as IAVI cohort) and **(B)** a UK cohort; here data are shown split by cohort (pooled data are shown in Fig. 3E).

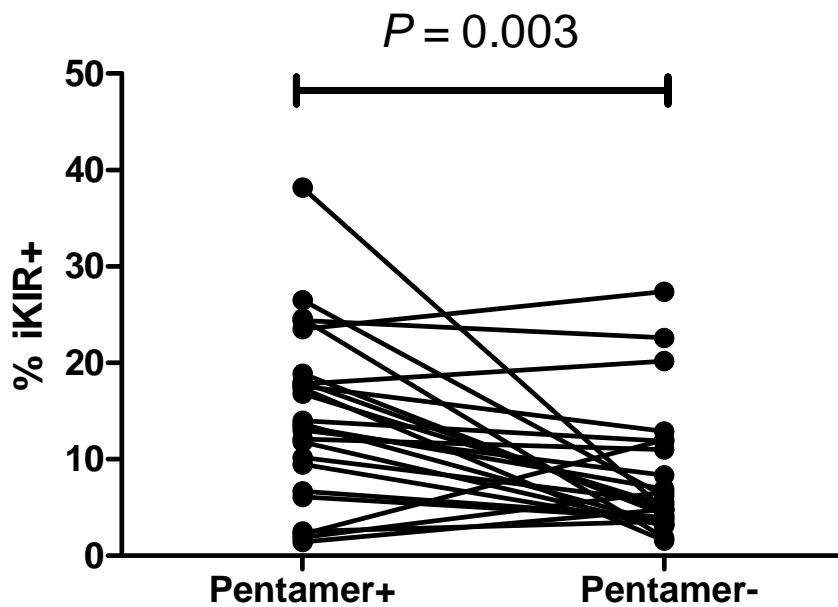


Figure S8: iKIR expression on pentamer-positive and pentamer-negative cells

The percentage of cells that express iKIR in the pentamer+ and pentamer- populations (gated on memory CD8+CD3+ cells) was quantified.

We have included this data for completeness but please note, interpretation is problematic since, whilst the “pentamer+” population will be a pure population of cells specific for HIV-1 or HTLV-1 the “pentamer-“ population will be a mixture consisting of cells specific for HIV-1 and HTLV-1 (but recognising other epitopes and HLA) and cells specific for other antigens.

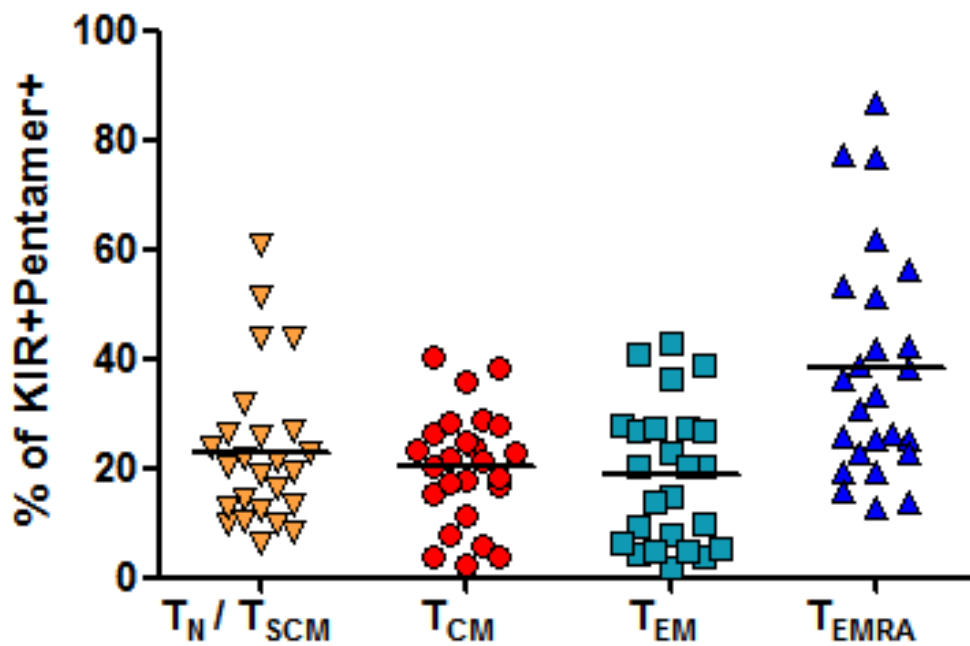


Figure S9: Differentiation stage of iKIR⁺ pentamer⁺ CD8⁺ T cells

The differentiation stage of iKIR⁺ pentamer⁺ CD8⁺ T cells from HIV-1 (N=16) and HTLV-1 (N=9) seropositive subjects was assessed by CD28 and CD45RA costaining. Abbreviations- T_N/T_{SCM} : T naïve/ T stem cell memory (CD45RA⁺CD28⁺); T_{CM} : T central memory (CD45RA⁻CD28⁺), T_{EM} : T effector memory (CD45RA⁻CD28⁻), T_{EMRA} : T effector memory revertant (CD28⁻CD45RA⁺).

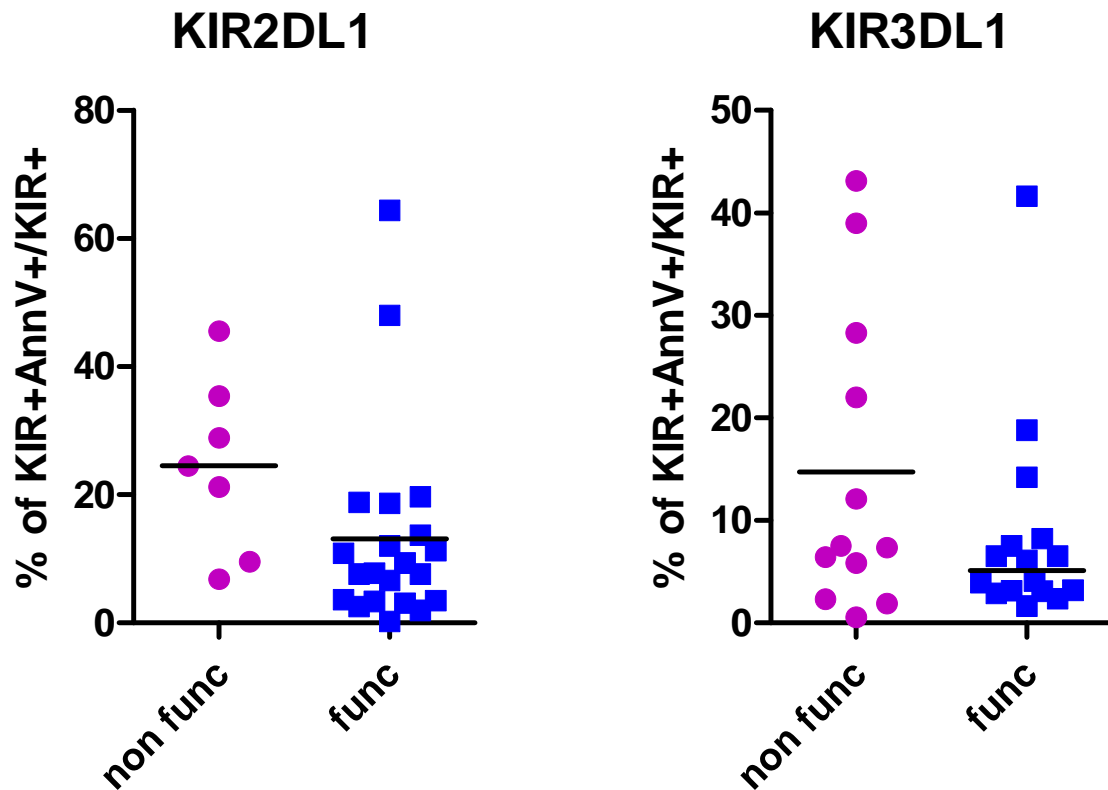
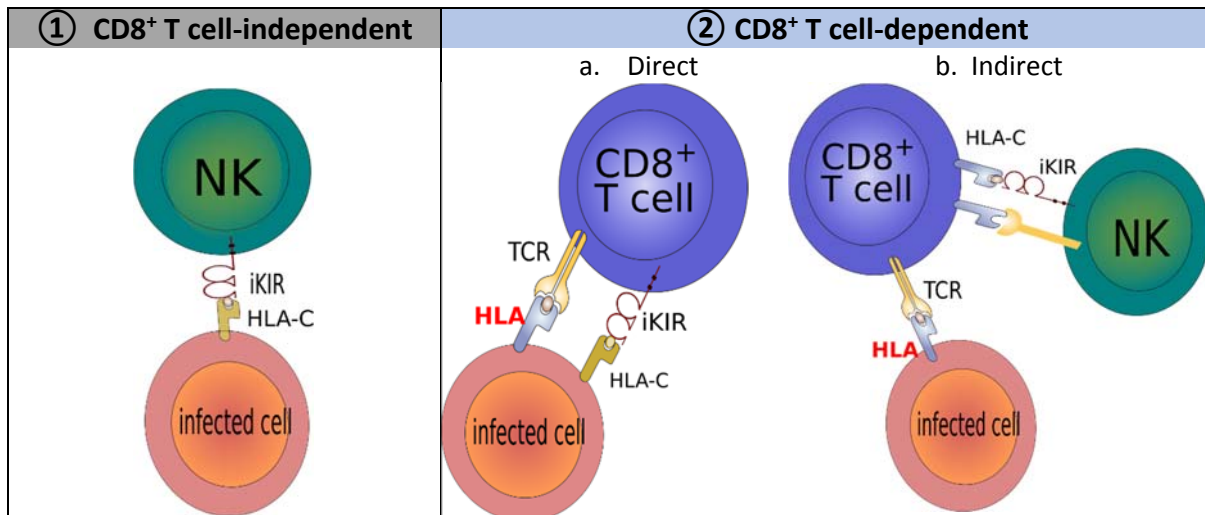


Figure S10: Annexin V binding to iKIR⁺ CD8⁺ T cells is decreased in individuals carrying the KIR ligand.

The proportion of KIR2DL1-expressing (left) and KIR3DL1-expressing (right) CD8⁺ T cells that bound Annexin V directly *ex vivo* was quantified. Data were split depending on whether the gene for the HLA ligand was absent in that individual (“non-func”) or present (“func”). KIR2DL2/L3 could not be analysed as there were only 2/30 individuals with non-functional KIR2DL2/L3. For KIR2DL1 we found that Annexin V binding was significantly decreased in people with the ligand ($P=0.027$, WMW), for KIR3DL1 there was a trend in the same direction but the difference was not significant. Combining P values we found $P=0.014$ (Stouffer’s weighted z-test); suggesting that presence of the KIR ligand was associated with a small reduction in cell death amongst KIR-expressing CD8⁺ T cells.

A.



B.

PREDICTION		OBSERVATION
① CD8 ⁺ T cell-independent	② CD8 ⁺ T cell-dependent	
Hypothesis: iKIR enhance HLA class I associations because they enhance antiviral NK cells	Hypothesis: iKIR enhance HLA class I associations because they enhance antiviral CD8 ⁺ T cells	
iKIR with ligands would affect outcome	iKIR with ligands would have no direct effect on outcome	iKIR with ligands have no direct effect on outcome (Table S2)
Only HLA molecules that bind KIR would be enhanced	HLA effects would be enhanced independent of whether iKIR bind the HLA	HLA effects are enhanced independent of whether iKIR bind the HLA (Table 2)
Primary HLA associations would be attributable to NK cells	Primary HLA associations would be attributable to CD8 ⁺ T cells	Primary HLA associations are more likely to be due to CD8 ⁺ T cells (Table S10)

Figure S11: Schematic and predictions of possible hypotheses

(A) *A priori* the immunogenetics data, which shows that iKIR enhance protective and detrimental HLA class I associations could be ① due to enhancement of NK cell-mediated control of virus infection i.e. be CD8⁺ T cell-independent or ② could be due to enhancement of CD8⁺ T cell-mediated control of virus infection i.e. be CD8⁺ T cell-dependent. (B) The table summarises predictions of both hypotheses and compares them with observation. The data are more consistent with the CD8⁺ T cell-dependent hypothesis. This does not rule out the occurrence of CD8⁺ T cell-independent processes in the viral infection; indeed both the *KIR3DS1:Bw4_80I* and *KIR2DL3:C1* associations in HIV-1 and HCV respectively, are consistent with a CD8⁺ T cell-independent mechanism (and satisfy all predictions in column ①), but our observations are in addition to, and independent of, these results.

Within hypothesis ② (CD8⁺ T cell-dependent) a number of ways in which iKIRs can increase CD8⁺ T cell survival have been described. These can be broadly divided into a) “direct” (iKIRs on T cells affect T cell lifespan, and b) “indirect” (iKIRs on other cell populations, e.g. NK cells,

affect T cell lifespan. We find evidence that, *in vitro*, iKIR expression on CD8⁺ T cells is directly associated with increased survival; this does not preclude a role for iKIR on NK cells in also indirectly enhancing CD8⁺ T cell survival. Both effects may be occurring and increasing CD8⁺ T cell survival and both are consistent with our immunogenetics analysis, the longitudinal study and the mathematical modelling. In short hypothesis ① (CD8⁺ T cell-independent) is inconsistent with the data; hypothesis ② (CD8⁺ T cell-dependent either direct or indirect) is consistent with the data.

Supplementary Tables

A. IAVI - EARLY VIRAL LOAD (whole cohort)					
KIR gene	Ligand gene	Coefficient	P value	N carriers	N non-carriers
<i>KIR3DL1</i>	<i>HLA-B Bw4</i>	-0.15	0.07 .	378	172
<i>KIR3DL1</i>	<i>HLA-B Bw4-80I</i>	-0.05	0.5	327	226
<i>KIR3DL1</i>	<i>HLA-A & -B Bw4</i>	-0.06	0.5	413	137
<i>KIR3DL1</i>	<i>HLA-A & -B Bw4-80I</i>	+0.07	0.4	376	176
<i>KIR3DS1</i>	<i>HLA-B Bw4</i>	-0.29	0.007 **	75	475
<i>KIR3DS1</i>	<i>HLA-B Bw4-80I</i>	-0.28	0.01 *	66	486
<i>KIR3DS1</i>	<i>HLA-A & -B Bw4</i>	-0.23	0.02 *	85	465
<i>KIR3DS1</i>	<i>HLA-A & -B Bw4-80I</i>	-0.20	0.06 .	77	474
B. IAVI - TIME TO LOW CD4 COUNT (whole cohort)					
KIR gene	Ligand gene	HR	P value	N carriers	N non-carriers
<i>KIR3DL1</i>	<i>HLA-B Bw4</i>	0.91	0.5	405	186
<i>KIR3DL1</i>	<i>HLA-B Bw4-80I</i>	1.02	0.9	353	241
<i>KIR3DL1</i>	<i>HLA-A & -B Bw4</i>	1.04	0.8	442	149
<i>KIR3DL1</i>	<i>HLA-A & -B Bw4-80I</i>	1.21	0.2	404	189
<i>KIR3DS1</i>	<i>HLA-B Bw4</i>	0.66	0.05 .	84	507
<i>KIR3DS1</i>	<i>HLA-B Bw4-80I</i>	0.64	0.05 *	75	518
<i>KIR3DS1</i>	<i>HLA-A & -B Bw4</i>	0.76	0.14	95	496
<i>KIR3DS1</i>	<i>HLA-A & -B Bw4-80I</i>	0.77	0.19	87	505

Table S1: Impact of *KIR3DS1* and *KIR3DL1* in the full IAVI cohort.

The impact of functional *KIR3DS1* and functional *KIR3DL1* in the full cohort on early viral load set point (A) and time to low CD4⁺ count (B) was quantified. The ligands of *KIR3DL1* are known to be HLA-B alleles bearing the Bw4 epitope, it is unclear whether the Bw4-80I/T dimorphism affects binding (78); additionally it is unclear whether HLA-A alleles bearing the Bw4 epitope are also ligands. We therefore considered four different definitions of functional *KIR3DL1*: *KIR3DL1-Bw4* (HLA-B alleles only), *KIR3DL1-Bw4-80I* (HLA-B alleles only), *KIR3DL1-Bw4* (HLA-A and -B alleles), *KIR3DL1-Bw4-80I* (HLA-A and B-alleles). The ligands of *KIR3DS1* have not

been fully established. One study demonstrated that KIR3DS1 can bind HLA-B57 (a Bw4-80I allele) (79) and immunogenetic evidence (31) suggests that, at least in the context of HIV-1 infection, HLA-Bw4-80I serves as a ligand for KIR3DS1. Based on this and the structural similarity of the extracellular domain to KIR3DL1 we again consider 4 possible definitions of functional KIR3DS1: *KIR3DS1-Bw4* (HLA-B alleles only), *KIR3DS1-Bw4-80I* (HLA-B alleles only), *KIR3DS1-Bw4* (HLA-A and -B alleles), *KIR3DS1-Bw4-80I* (HLA-A and -B alleles). It has also been shown that KIR3DS1 binds the non-classical HLA molecule HLA-F, which is carried by everyone. There is no evidence that this confers protection since KIR3DS1 in a Bw4⁻ cohort is not protective ($P=0.18$). For viral load set point a negative coefficient represents protection (a decrease in viral load associated with the gene combination) for time to low CD4 a hazard ratio (HR) less than 1 represents protection (a decrease in the relative risk of progression associated with the gene combination). It can be seen that KIR3DL1 does not confer protection (with any of its possible ligands) whereas KIR3DS1 with its putative HLA B ligands does confer protection.

Functional *KIR3DL1* (*KIR3DL1-HLA-Bw4*) has previously been associated with good NK cell mediated-control of HIV-1 infection (23, 76). This protective effect was seen for all *KIR3DL1* alleles, but was strongest for alleles with high surface expression (*001, *002, *008, *015, *009) and very low/no surface expression (*004) (80). It is therefore particularly surprising that the protective effect of *KIR3DL1* was not replicated in the IAVI cohort which would be expected to be heavily enriched for the high expressing alleles *KIR3DL1**001 and *015 (23, 81).

A. IAVI - EARLY VIRAL LOAD					
KIR	Ligands	Coefficient	P value	N carriers	N non-carriers
<i>KIR2DL1</i>	C2	0.06	0.5	326	135
<i>KIR2DL2</i>	C1, C2	-0.01	0.9	291	170
<i>KIR2DL2</i>	C1	-0.09	0.3	188	273
<i>KIR2DL3</i>	C1	-0.15	0.06	263	198
<i>KIR3DL1</i>	HLA-B Bw4	-0.07	0.4	245	216
Inhibitory Score (continuous)	NA	-0.07	0.2	NA	NA
Inhibitory Score (cut off = 2.0)	NA	-0.09	0.3	252	209
Inhibitory Score (cut off = 2.5)	NA	-0.12	0.1	182	279
Count Func iKIR (cut off = 2.0)	NA	-0.09	0.3	252	209
B. IAVI - TIME TO LOW CD4 COUNT					
KIR	Ligands	HR	P value	N carriers	N non-carriers
<i>KIR2DL1</i>	C2	1.18	0.3	349	142
<i>KIR2DL2</i>	C1, C2	0.98	0.9	306	185
<i>KIR2DL2</i>	C1	0.96	0.8	197	294
<i>KIR2DL3</i>	C1	1.00	1.0	278	213
<i>KIR3DL1</i>	HLA-B Bw4	0.96	0.8	311	180
Inhibitory Score (continuous)	NA	1.03	0.8	NA	NA
Inhibitory Score (cut off = 2.0)	NA	0.91	0.5	263	228
Inhibitory Score (cut off = 2.5)	NA	0.93	0.6	190	301
Count Func iKIR (cut off=2.0)	NA	1.00	1.0	263	228
C. KAGOSHIMA – ODDS OF DISEASE (HAM/TSP)					
KIR	Ligands	OR	P value	N carriers	N non-carriers
<i>KIR2DL1</i>	C2	1.19	0.7	39	353
<i>KIR2DL2</i>	C1, C2	0.90	0.7	100	292
<i>KIR2DL2</i>	C1	0.89	0.7	99	293
<i>KIR2DL3</i>	Insufficient Functional 2DL3 ⁺ subjects				
<i>KIR3DL1</i>	HLA-B Bw4	1.21	0.5	197	195
Inhibitory Score (continuous)	NA	1.06	0.7	NA	NA
Inhibitory Score (cutoff=1.5)	NA	1.50	0.2	262	130
Inhibitory Score (cut off=1.75)	NA	0.67	0.2	66	326

Count Functional iKIR (cut off=1)	NA	1.53	0.1	263	129
D. HCV – ODDS OF SPONTANEOUS CLEARANCE					
KIR	Ligands	OR	P value	N carriers	N non-carriers
<i>KIR2DL1</i>	C2	0.74	0.08	519	262
<i>KIR2DL2</i>	C1, C2	0.86	0.3	408	374
<i>KIR2DL2</i>	C1	0.90	0.5	332	450
<i>KIR2DL3</i>	C1	1.55	0.02 *	562	220
<i>KIR3DL1</i>	HLA-B Bw4	1.06	0.7	485	297
Inhibitory Score (continuous)	NA	0.97	0.7	NA	NA
Inhibitory Score (cut off=2.0)	NA	0.99	1.0	415	366
Inhibitory Score (cut off=2.5)	NA	0.97	0.8	365	416
Inhibitory Score (cut off=2.75)	NA	0.79	0.3	120	661
Count Functional iKIR (cut off=2)	NA	0.99	1.0	415	366
E. HCV – ODDS OF SPONTANEOUS CLEARANCE with <i>KIR2DL3:C1</i> as a covariate					
KIR	Ligands	OR	P value	N carriers	N non-carriers
<i>KIR2DL1</i>	C2	0.8	0.2	519	262
<i>KIR2DL2</i>	C1, C2	0.92	0.6	408	374
<i>KIR2DL2</i>	C1	0.85	0.3	332	450
<i>KIR2DL3</i>	C1	1.00	1.0	562	220
<i>KIR3DL1</i>	HLA-B Bw4	1.11	0.5	485	297
Inhibitory Score (continuous)	NA	0.93	0.4	NA	NA
Inhibitory Score (cut off=2.0)	NA	0.91	0.6	415	366
Inhibitory Score (cut off=2.5)	NA	0.80	0.2	365	416
Inhibitory Score (cut off=2.75)	NA	0.77	0.3	120	661
Count Functional iKIR (cut off=2)	NA	0.91	0.6	415	366

Table S2: Influence of individual functional iKIRs, Inhibitory Score and count of Functional Inhibitory KIRs alone.

(A) Early viral load set point in IAVI. **(B)** Time to low CD4⁺ cell count in IAVI. **(C)** Odds of HTLV-1 associated disease (HAM/TSP) in Kagoshima **(D)** Odds of spontaneous clearance of HCV **(E)**

Odds of spontaneous clearance of HCV with *KIR2DL3:C1* as a covariate. It can be seen that with the exception of Functional *2DL3* in HCV (reported (27)) none of the iKIRs alone with their ligands (i.e. without also including protective or detrimental HLA alleles) have a significant impact on the outcome measures.

A: Linear regression, covariates: gender. B Cox regression, covariates: age at infection and site. C: Logistic regression: covariates: age and gender. D: Logistic regression: covariates: age and gender. E: Logistic regression: covariates: age, gender and *KIR2DL3:C1*.

C1 ligands includes HLA-B*46 & HLA-B*73, NA: not applicable. For Inhibitory scores or Count Functional iKIR, the number of carriers designates the number of subjects with the score/count greater than the cut-off.

A. EARLY VIRAL LOAD								
	<i>B57⁺ KIR⁻</i>		<i>B57⁺ KIR⁺</i>		Cohort numbers			
	Coeff	P value	Coeff	P value	<i>B57⁺ KIR⁻</i>	<i>B57⁻ KIR⁻</i>	<i>B57⁺ KIR⁺</i>	<i>B57⁻ KIR⁺</i>
Functional <i>2DL1</i>	-0.20	0.4	-0.51	0.003**	10	125	25	301
Functional <i>2DL2</i> (strong)	-0.31	0.1	-0.68	0.01*	17	153	10	178
Functional <i>2DL2</i> (weak)			-0.34	0.2			8	95
Functional <i>2DL3</i>	-0.19	0.3	-0.67	0.001**	18	180	17	246
Inhibitory score (cutoff=2)	-0.17	0.4	-0.59	0.002**	14	195	21	231
Inhibitory score (cutoff=2.5)	-0.27	0.15	-0.65	0.004**	21	258	14	168
Count functional iKIR (cutoff=2)	-0.17	0.4	-0.59	0.002**	14	195	21	231
B. TIME TO LOW CD4 COUNT								
	<i>B57⁺ KIR⁻</i>		<i>B57⁺ KIR⁺</i>		Cohort numbers			
	HR	P value	HR	P value	<i>B57⁺ KIR⁻</i>	<i>B57⁻ KIR⁻</i>	<i>B57⁺ KIR⁺</i>	<i>B57⁻ KIR⁺</i>
Functional <i>2DL1</i>	0.60	0.4	0.39	0.02*	10	132	25	324
Functional <i>2DL2</i> (strong)	0.31	0.05*	0.29	0.09	17	168	10	187
Functional <i>2DL2</i> (weak)			1.01	0.98			8	101
Functional <i>2DL3</i>	0.53	0.12	0.33	0.06	18	195	17	261
Inhibitory score (cutoff=2)	0.48	0.15	0.42	0.05	14	214	21	242
Inhibitory score (cutoff=2.5)	0.57	0.15	0.25	0.05*	21	280	14	176
Count functional iKIR (cutoff = 2)	0.48	0.15	0.42	0.05	14	214	21	242

Table S3: Functional iKIRs enhance the protective effect of *HLA-B*57*, analysis by factor.

We repeated our calculations using an alternative statistical approach. Rather than stratify the cohort and then analyse the effect of *HLA-B*57* in each stratum we worked with the unstratified cohort and introduced a factor with three levels: *HLA-B*57⁻* (baseline); *HLA-B*57⁺ KIR⁻* and *HLA-B*57⁺ KIR⁺* where KIR was one of functional *KIR2DL1*, functional

KIR2DL2, functional *KIR2DL3*, high inhibitory score or high count of functional iKIR. **(A)**

Outcome variable: early viral load set point. Multivariate linear regression was performed on the unstratified IAVI cohort. The coefficient and p value of the factor levels are reported **(B)**

Outcome variable: time to low CD4⁺ count Multivariate Cox regression was performed on the unstratified cohort. Confounding factors were age at infection and site, the dependent variable was the factor based on presence and absence of KIR and *HLA-B*57* as described above. Hazard ratios (HR) and p values are reported.

It can be seen that for both outcomes, *HLA-B*57* without the functional iKIR is not significantly protective but in combination with the functional iKIR *HLA-B*57* is significant protective consistent with our findings using the alternative stratification approach.

IAVI early viral load set point		
	Coeff	P value
LILRB2_A	-0.02	0.9
LILRB2_B	+0.53	0.001 **
LILRB2_C	-0.16	0.2
LILRB2_all	+0.37	0.008 **

Table S4. Impact of LILRB2 –HLA class I binding on early viral load set point in IAVI

The LILRB2_B score (**Supplementary Methods**), which is the sum of the binding affinities of LILRB2 to the HLA-B alleles, is significantly detrimental. The LILRB2_A and _C scores (binding to the HLA-A and HLA-C molecules) did not significantly influence the early viral load set point. A combined score (**Supplementary Methods**) for the three HLA loci was also significantly detrimental but is likely to be driven by the LILRB2_B score.

A. EARLY VIRAL LOAD (with extra confounder: LILRB2_B)								
	<i>B57⁺ KIR⁻</i>		<i>B57⁺ KIR⁺</i>		Cohort numbers			
	Coeff	P value	Coeff	P value	<i>B57⁺ KIR⁻</i>	<i>B57⁻ KIR⁻</i>	<i>B57⁺ KIR⁺</i>	<i>B57⁻ KIR⁺</i>
Functional <i>2DL1</i>	-0.11	0.7	-0.47	0.009**	10	123	25	294
Functional <i>2DL2</i> (strong)			-0.55	0.03*			10	174
Functional <i>2DL2</i> (weak)	-0.26	0.2	-0.53	0.02*	17	148	15	205
Functional <i>2DL3</i>	-0.22	0.3	-0.54	0.008**	18	178	17	239
Inhibitory score (cutoff=2)	-0.14	0.5	-0.52	0.008**	14	193	21	224
Inhibitory score (cutoff=2.5)	-0.25	0.17	-0.53	0.02*	21	256	14	161
Count iKIR (cutoff=2)	-0.14	0.5	-0.52	0.008**	14	193	21	224
B. EARLY VIRAL LOAD (with extra confounder: Func 3DL1)								
	<i>B57⁺ KIR⁻</i>		<i>B57⁺ KIR⁺</i>		Cohort numbers			
	Coeff	P value	Coeff	P value	<i>B57⁺ KIR⁻</i>	<i>B57⁻ KIR⁻</i>	<i>B57⁺ KIR⁺</i>	<i>B57⁻ KIR⁺</i>
Functional <i>2DL1</i>	-0.11	0.7	-0.51	0.005**	10	125	25	301
Functional <i>2DL2</i> (strong)			-0.59	0.03*			10	178
Functional <i>2DL2</i> (weak)	-0.29	0.13	-0.56	0.02*	17	153	15	208
Functional <i>2DL3</i>	-0.24	0.3	-0.58	0.004**	18	180	17	246
Inhibitory score (cutoff=2)	-0.16	0.5	-0.55	0.005**	14	195	21	231
Inhibitory score (cutoff=2.5)	-0.27	0.15	-0.57	0.01*	21	258	14	168
Count iKIR (cutoff=2)	-0.16	0.5	-0.55	0.005**	14	195	21	231

Table S5: Functional iKIRs enhance the protective effect of *HLA-B*57* on early set point viral load, even when *LILRB2_B* binding score and Functional *KIR3DL1* are included.

The IAVI cohort was stratified into individuals with and without the functional iKIR of interest, by inhibitory score and by count of functional iKIR. In each of the strata the protective effect of *HLA-B*57* on early viral set point was estimated, after the effects of (A) *LILRB2_B* binding score or (B) Functional *KIR3DL1* were regressed out, together with the effect of gender.

IAVI EARLY VIRAL LOAD								
	<i>B35Px⁺ KIR⁻</i>		<i>B35Px⁺ KIR⁺</i>		Cohort numbers			
	Coeff	P value	Coeff	P value	<i>B35Px⁺ KIR⁻</i>	<i>B35Px⁻ KIR⁻</i>	<i>B35Px⁺ KIR⁺</i>	<i>B35Px⁻ KIR⁺</i>
Functional 2DL1	0.63	0.01*	0.3	0.01**	9	126	69	257
Functional 2DL2 (strong)			0.11	0.6			23	165
Functional 2DL2 (weak)	0.45	0.004**	0.28	0.05*	28	141	48	175
Functional 2DL3	0.3	0.03*	0.36	0.02*	48	150	30	233
Inhibitory score (cut-off=2.0)	0.32	0.08.	0.41	0.001**	20	189	58	194
Inhibitory score (cut-off=2.5)	0.40	0.003**	0.29	0.07.	46	233	32	150
Count Func iKIR (cut-off = 2)	0.32	0.08.	0.41	0.001**	20	189	58	194

Table S6: Functional iKIRs have no clear impact on the detrimental effect of *HLA-B*35Px* on viral load set-point in the IAVI cohort.

We stratified the IAVI cohort based on the iKIR score (with two different cut-offs) and based on the count of iKIRs. In each stratum we analysed the strength of the detrimental *HLA-B*35Px* effect. The results were inconsistent and we conclude that there is no clear evidence that iKIRs enhance the detrimental effect of *HLA-B*35Px* on early viral set-point in the IAVI cohort.

Definitions: Functional 2DL1: *KIR2DL1⁺C2⁺*. Functional 2DL2 (strong): *KIR2DL2⁺C1⁺*. Functional 2DL2 (weak): *KIR2DL2⁺C2⁺*. Functional 2DL3: *KIR2DL3⁺C1⁺*. Inhibitory score (cut-off=2.0): inhibitory score>2.0. Inhibitory score (cut-off=2.5): inhibitory score>2.5. Count (cut-off=2.0): count of functional iKIR>2.0.

A. US HLA-B*57		time to CD4<200 (with extra covariate <i>KIR3DL1_h/y+Bw4-80I</i>)						
	<i>B57+ KIR⁻</i>		<i>B57+ KIR⁺</i>		Cohort numbers			
	HR	P value	HR	P value	<i>B57+ KIR⁻</i>	<i>B57- KIR⁻</i>	<i>B57+ KIR⁺</i>	<i>B57- KIR⁺</i>
Inhibitory score (cutoff=2)	0.25	0.18	0.27	0.006 **	8	236	36	210
Inhibitory score (cutoff=2.5)	0.38	0.19	0.24	0.01 *	11	271	33	175
B. US HLA-B*35Px		time to CD4<200 (with extra covariate <i>KIR3DL1_h/y+Bw4-80I</i>)						
	<i>B35Px+ KIR⁻</i>		<i>B35Px+ KIR⁺</i>		Cohort numbers			
	HR	P value	HR	P value	<i>B35Px+ KIR⁻</i>	<i>B35Px- KIR⁻</i>	<i>B35Px+ KIR⁺</i>	<i>B35Px- KIR⁺</i>
Inhibitory score (cutoff=2)	1.33	0.43	2.71	0.001 **	20	224	44	202
Inhibitory score (cutoff=2.5)	1.75	0.04 *	2.41	0.01 *	37	245	27	181

Table S7: Impact of Functional iKIRs on the effect of *HLA-B*57* and *HLA-B*35Px* in the US cohort when *KIR3DL1_h/y+Bw4-80I* is included as a covariate.

It has previously been shown that the level of *KIR3DL1* expression impacts on time to low CD4⁺ cell count with high expressing *KIR3DL1* alleles plus *HLA-Bw4-80I* associated with slow progression (**23**). We therefore repeated our analysis with *KIR3DL1_h/y+Bw4-80I* included as a covariate. Conclusions were unchanged.

<i>HLA</i>	Odds Ratio	P-value	Cohort size	
			<i>HLA +</i>	<i>HLA-</i>
<i>HLA-A*02</i>	0.43	0.001 **	150	242
<i>HLA-A*02:01</i>	0.72	0.4	49	343
<i>HLA-A*02:06</i>	0.58	0.09 .	74	318
<i>HLA-A*02:07</i>	0.28	0.008 **	30	362

Table S8: The protective effect of *HLA-A*02* on odds of HAM/TSP in the Kagoshima cohort is driven by *HLA-A*02:07*.

Logistic regression with age and gender as confounding factors. The protection (decreased odds ratio) associated with *HLA-A*02* is largely attributable to *HLA-A*02:07*, not the more frequent *HLA-A*02:01* and *HLA-A*02:06* alleles which do not reach significance despite their increased frequency.

HLA-B*57 (without Functional 2DL3 as confounder)								
	<i>B57⁺ KIR⁻</i>		<i>B57⁺ KIR⁺</i>		Cohort numbers			
	OR	P value	OR	P value	<i>B57⁺ KIR⁻</i>	<i>B57⁻ KIR⁻</i>	<i>B57⁺ KIR⁺</i>	<i>B57⁻ KIR⁺</i>
Functional 2DL2 (strong)			2.91	0.009**			31	301
Functional 2DL2 (weak)	1.20	0.6	2.63	0.01*	35	339	43	220
Functional 2DL3	1.90	0.13	1.82	0.06	38	182	46	516
Inhibitory score (cut off=2.5)	1.55	0.3	2.04	0.03*	34	382	50	315
Inhibitory score (cut off=2.75)	1.50	0.15	4.20	0.009**	60	601	24	96
Count iKIR (cut off=2)	1.26	0.7	2.02	0.02*	19	347	65	350
Count iKIR (cut off=3)	1.49	0.15	6.25	0.0098**	67	621	17	76
HLA-B*57 (with Functional 2DL3 as confounder)								
	<i>B57⁺ KIR⁻</i>		<i>B57⁺ KIR⁺</i>		Cohort numbers			
	OR	P value	OR	P value	<i>B57⁺ KIR⁻</i>	<i>B57⁻ KIR⁻</i>	<i>B57⁺ KIR⁺</i>	<i>B57⁻ KIR⁺</i>
Functional 2DL2 (strong)			3.08	0.006**			31	301
Functional 2DL2 (weak)	1.29	0.5	2.89	0.008**	35	339	43	220
Functional 2DL3	1.90	0.1	1.82	0.06	38	182	46	516
Inhibitory score (cut off=2.5)	2.16	0.06	2.16	0.02*	34	382	50	315
Inhibitory score (cut off=2.75)	1.69	0.08	4.43	0.008**	60	601	24	96
Count iKIR (cut off=2)	1.83	0.3	2.12	0.01*	19	347	65	350
Count iKIR (cut off=3)	1.72	0.05	6.25	0.0098**	67	621	17	76

Table S9: The protective effect of HLA-B*57 on odds of spontaneous clearance of HCV is enhanced with increasing inhibitory scores.

Logistic regression with confounding factors mode of infection, HBV serostatus, SNP rs12979860, in subcohorts stratified by KIR.

A. IAVI - EARLY VIRAL LOAD						
KIR gene	Ligand gene	Coeff	Prot/det	P value	N carriers	N non-carriers
<i>KIR3DL1</i>	<i>HLA-B Bw4</i>	-0.07	P	0.4	294	167
<i>KIR3DL1</i>	<i>HLA-B Bw4-80I</i>	+0.02	D	0.8	245	216
<i>KIR3DL1</i>	<i>HLA-A & -B Bw4</i>	+0.01	D	0.9	327	134
<i>KIR3DL1</i>	<i>HLA-A & -B Bw4-80I</i>	+0.12	D	0.1	291	170
B. IAVI - TIME TO LOW CD4 COUNT						
KIR gene	Ligand gene	HR	Prot/det	P value	N carriers	N non-carriers
<i>KIR3DL1</i>	<i>HLA-B Bw4</i>	0.96	P	0.8	311	180
<i>KIR3DL1</i>	<i>HLA-B Bw4-80I</i>	1.07	D	0.6	261	230
<i>KIR3DL1</i>	<i>HLA-A & -B Bw4</i>	1.10	D	0.5	346	145
<i>KIR3DL1</i>	<i>HLA-A & -B Bw4-80I</i>	1.27	D	0.1	309	182
C. IAVI - EARLY VIRAL LOAD excluding HLA-B*57+ individuals from cohort						
KIR gene	Ligand gene	Coeff	Prot/det	P value	N carriers	N non-carriers
<i>KIR3DL1</i>	<i>HLA-B Bw4</i>	-0.02	P	0.8	259	167
<i>KIR3DL1</i>	<i>HLA-B Bw4-80I</i>	+0.08	D	0.3	210	216
<i>KIR3DL1</i>	<i>HLA-A & -B Bw4</i>	+0.06	D	0.5	292	134
<i>KIR3DL1</i>	<i>HLA-A & -B Bw4-80I</i>	+0.18	D	0.03	256	170
D. IAVI - TIME TO LOW CD4 COUNT excluding HLA-B*57+ individuals from cohort						
KIR gene	Ligand gene	HR	Prot/det	P value	N carriers	N non-carriers
<i>KIR3DL1</i>	<i>HLA-B Bw4</i>	1.1	D	0.8	276	180
<i>KIR3DL1</i>	<i>HLA-B Bw4-80I</i>	1.2	D	0.2	226	230
<i>KIR3DL1</i>	<i>HLA-A & -B Bw4</i>	1.2	D	0.2	311	145
<i>KIR3DL1</i>	<i>HLA-A & -B Bw4-80I</i>	1.4	D	0.03	274	182
E. KAGOSHIMA – ODDS OF DISEASE (HAM/TSP)						
KIR gene	HLA gene	OR	Prot/det	P value	N carriers	N non-carriers
-	<i>A*11:01</i>	1.1	D	0.75	324	68
-	<i>A*02:07</i>	0.3	P	0.008	362	30
-	<i>A*02:06</i>	0.6	P	0.09	318	74
-	<i>A*31:01</i>	1.5	D	0.25	322	70
-	<i>A*02:01</i>	0.7	P	0.4	343	49
-	<i>A*33:03</i>	1.2	D	0.72	344	48
-	<i>A*26:01</i>	1.0	D	0.91	321	71
F. KAGOSHIMA – ODDS OF DISEASE (HAM/TSP)						

KIR gene	HLA gene	OR	Prot/det	P value	N carriers	N non-carriers
-	<i>C*01</i>	1.32	D	0.29	223	169
-	<i>C*03</i>	0.56	P	0.03	209	183
-	<i>C*07</i>	1.22	D	0.51	299	93
-	<i>C*08</i>	0.50	P	0.06	336	56
-	<i>C*12</i>	0.87	P	0.66	312	80
-	<i>C*14</i>	1.63	D	0.12	306	86

G. KAGOSHIMA – ODDS OF DISEASE (HAM/TSP)						
KIR gene	HLA gene	OR	Prot/det	P value	N carriers	N non-carriers
-	<i>B*07</i>	1.49	D	0.27	336	56
-	<i>B*54</i>	2.61	D	0.006	310	82
-	<i>B*46</i>	0.62	P	0.23	344	48
-	<i>B*35</i>	0.80	P	0.53	340	52
-	<i>B*40</i>	0.69	P	0.18	260	132
-	<i>B*07</i>	1.49	D	0.27	336	56

H. HCV– ODDS OF SPONTANOUS CLEARANCE						
KIR gene	HLA gene	OR	Prot/det	P value	N carriers	N non-carriers
<i>KIR3DL1</i>	<i>HLA-B Bw4</i>	1.06	P	0.72	485	297
<i>KIR3DL1</i>	<i>HLA-B Bw4-80I</i>	1.13	P	0.46	291	491
<i>KIR3DL1</i>	<i>HLA-A & -B Bw4</i>	0.97	D	0.86	551	231
<i>KIR3DL1</i>	<i>HLA-A & -B Bw4-80I</i>	1.05	P	0.76	421	361

I. HCV– ODDS OF SPONTANOUS CLEARANCE						
KIR gene	HLA gene	OR	Prot/det	P value	N carriers	N non-carriers
<i>KIR3DS1</i>	<i>HLA-B Bw4</i>	1.08	P	0.70	159	623
<i>KIR3DS1</i>	<i>HLA-B Bw4-80I</i>	1.24	P	0.38	91	691
<i>KIR3DS1</i>	<i>HLA-A & -B Bw4</i>	1.00	-	0.98	181	601
<i>KIR3DS1</i>	<i>HLA-A & -B Bw4-80I</i>	1.08	P	0.72	137	645

Table S10: Can the HLA class I associations studied be explained by NK-cell mediated effects?

If an HLA class I association is attributable to NK cells then other HLA class I molecules with similar KIR binding properties would (in the context of the relevant KIRs) be expected to be

similarly protective/detrimental. This behaviour was investigated for each of the six HLA class I associations that we studied.

Note *HLA-C*03* (which has a significantly protective impact on disease status in the Kagoshima cohort) was not included in the KIR analysis for HTLV-1 as we restricted our analysis to HLA associations that had been independently replicated; *HLA-C*03* did not meet this criterion.

A schematic summarising the hypotheses that could explain the observations is presented in **Fig. S11**.

Parameter	Meaning	Range	Source
λ_1	CD4 ⁺ T cell production rate	0.2 – 10 cells/mm ³ /day	(82-84)
s_1	CD4 ⁺ T cell proliferation rate	0.1 cells/mm ³ /day	(82, 83, 85)
k_1	Density control on CD4 ⁺ T cell proliferation rate	1100 cells/mm ³	(82, 83, 85)
β	Infectious transmissibility	10 ⁻⁶ – 10 ⁻⁴ mm ³ /cell/day	(83-86)
μ_1	Uninfected CD4 ⁺ T cell death rate	0.01 – 0.1 /day	(82-84, 87)
d_1	Lysis rate of infected cells by more/less efficient CD8 ⁺ T cells	3x[0.002 – 0.03] /cell day 0.3x[0.002 – 0.03] /cell day	(88, 89)
d_2	Lysis rate of infected cells by average CD8 ⁺ T cells	0.002 – 0.03 /cell day	(83, 84)
μ_2	Infected CD4 ⁺ T cell death rate	0.1 – 1 /day	(82-85, 90)
ρ	Viral production rate	50-700 virions/cell day	(83, 84, 87)
k_2	Density control on CD8 ⁺ T cell proliferation rate	200 cells/mm ³	(82, 83, 85)
μ_3	Viral clearance rate	2 – 30 /day	(83, 84, 87, 90)
λ_2	CD8 ⁺ T cell production rate	10 ⁻³ – 1 cells/mm ³ /day	(82, 85)
S_2	CD8 ⁺ T cell proliferation rate in response to infected CD4 ⁺ T cells	0.001 – 0.04 /day	(82-85)
μ_4	CD8 ⁺ T cell death rate	0.01-0.05 /day	(82-85)

Table S11: Parameter ranges used in the mathematical model of host-pathogen dynamics.

HLA B-C Combination	Carrier frequency
<i>B*1503 C*0210</i>	0.193
<i>B*5301 C*0401</i>	0.187
<i>B*5802 C*0602</i>	0.163
<i>B*4201 C*1701</i>	0.141
<i>B*0702 C*0702</i>	0.128
<i>B*1510 C*0304</i>	0.106
<i>B*4501 C*1601</i>	0.094
<i>B*4501 C*0602</i>	0.09
<i>B*4901 C*0701</i>	0.073
<i>B*4403 C*0401</i>	0.065
<i>B*1402 C*0802</i>	0.061
<i>B*5801 C*0701</i>	0.047
<i>B*3501 C*0401</i>	0.045
<i>B*1503 C*0401</i>	0.043
<i>B*1801 C*0704</i>	0.041
<i>B*0801 C*0701</i>	0.041
<i>B*5801 C*0602</i>	0.039
<i>B*5301 C*0602</i>	0.039
<i>B*1503 C*0602</i>	0.039
<i>B*1302 C*0602</i>	0.037

Table S12: Most frequent *HLA B-C* combinations in the IAVI cohort

The frequency of people carrying the top 20 most common *HLA B-C* combinations is reported. The *HLA* sequencing data were not phased so we report genotypes rather than haplotypes (i.e. all 4 possible *HLA-B-HLA-C* combinations were considered for each individual).